# Phosphate Recovery from Sewage Sludge by Density Concentration



"All the human and animal manure which the world wastes, if returned to the land, instead of being thrown into the sea, would suffice to nourish the world."

VICTOR HUGO

# Phosphate Recovery from Sewage Sludge by Density Concentration

by

# S. Koomen

to obtain the degree of Master of Science in Applied Earth Sciences at the Delft University of Technology

August 2019

Student number: 4294750

Supervisors: Prof. dr. P.C. Rem TU Delft

W. Wijdeveld MSc Wetsus

Thesis committee: Prof. dr. P.C. Rem TU Delft, Resources & Recycling

Dr. M.C.M Bakker TU Delft, Resources & Recycling TU Delft, Resource Engineering

An electronic version of this thesis is available at <a href="http://repository.tudelft.nl/">http://repository.tudelft.nl/</a>.





# **Acknowledgements**

This report presents the theoretical and experimental research that I have performed as a master's thesis in Applied Earth Sciences at the Technical University of Delft. During this research, I investigated the feasibility of density concentration of ferro-phosphate minerals from digested sewage sludge. I would not have been able to do this research on my own, and therefore I would like to thank all that were involved personally.

First of all, I would like to thank Prof. dr. Peter Rem for giving me the opportunity to do this interesting research. I appreciate the time you made for our invaluable discussions and your support throughout this thesis. My gratitude also goes to Wokke Wijdeveld MSc., who supported me in many ways, from providing me with indispensable knowledge to assisting me during experiments. I want to thank Dr. Maarten Bakker and Dr. Mike Buxton for critically reviewing my work and giving me useful feedback. Thank you Stijn de Graaf, for the exceptional work you have done on spiral concentration with synthetic sludge.

Many thanks to Ing. Peter Berkhout, for all your patience and help, especially during the design of the experimental set-ups. Also all the support of Richard Idzes cannot be left unmentioned, thank you. I would like to thank Ron Penners for all his help and giving me the freedom to use all the equipment in the lab, or ordering new equipment whenever I needed it. I truly enjoyed the time I have spent with the Resources & Recycling staff, thank you all for making me a part of the team and offering me a working place in the office.

Last but not least, I would like to thank my friends and family for all their support during this project.

Stef Koomen Delft, August 2019

# **Abstract**

Phosphate is removed from wastewater to prevent eutrophication. Chemical phosphorus removal by iron dosing is commonly used for this purpose, where phosphorus is among others bound in the mineral vivianite ( $Fe(II)_3[PO_4]_2 \cdot 8 H_2O$ ). A molar Fe:P ratio of 2.5 in sludge will capture 70-90% of total phosphorus in vivianite after anaerobic digestion[58], a digestion method which offers ideal conditions for vivianite formation. Vivianite is paramagnetic, enabling it to be recovered by magnetic separation for recycling purposes. Phosphorus recycling from wastewater is of great importance, as in worst-case scenarios, 40-60% of all phosphate rock resources will be extracted by 2100[55]. It is furthermore estimated that in Europe 20-30% of the fertilizer demand can be met by using phosphorus that ends up in sludge in European sewage treatment plants[43].

To reduce processing costs of magnetic vivianite recovery, a pre-concentration step based on density concentration can be introduced, as vivianite particles are denser than organic material in sludge. This research investigated the feasibility of vivianite concentration from digested sewage sludge with a Multotec MX7 spiral concentrator. Spirals are applied in the mining industry for coal washing and pre-concentration of ores which are suspended in water. Particle separation on spirals is based on centrifugal and gravitational forces. Digested sewage sludge is more viscous than water, which affects the separation process on spiral concentrators. To investigate the influence of this high sludge viscosity on the spiral separation efficiency, laboratory experiments were performed.

A thin-film centrifuge was designed to investigate the particle migration behaviour in sewage sludge under a G-force of 245. The sludge contained 13% less solids and 23% less phosphorus after centrifuging, likely caused by minerals that attached to the centrifuge surface due to high friction forces. The first spiral experiments were performed with a viscous water-glycerol mixture, containing sand and PET particles, having similar densities to vivianite (2.65 g/cm<sup>3</sup>) and organic particles (1.40 g/cm<sup>3</sup>) in sewage sludge. Sand recoveries up to 90% were found with a product grade of 78%. An increase in feed rate showed a shift in particle size distribution, where fewer fine particles were recovered. The first experiment with digested sewage sludge, being more viscous than the synthetic sludge, showed no effective separation of vivianite and barely any concentration of solids. Samples were analyzed on total solids (TS) and volatile solids (VS) content, and on elemental composition with ICP-OES analysis. Samples were also taken from the third turn of the spiral (total of seven), where the solids concentration in the product was more than doubled compared to the feed. An additional experiment was performed with sewage sludge mixtures diluted with water. The viscosity of sludge dropped linearly with dilution. A decrease in viscosity increases the turbulence on the spiral, which improved the separation mechanism. Results showed that an increase in dilution decreases the volatile solids content in the product flow. Diluting the sludge furthermore improved the concentration of solids towards the product flow. However, spiral efficiencies were only 9%, while efficiencies over 80% were found for synthetic sludge, meaning that particle separation was limited. The iron concentration was highest in the product outlet and increased with dilution. The phosphorus content, however, was similar for all outlets and dilutions, suggesting that only Fe minerals other than vivianite, such as siderite and pyrite, concentrated towards the product flow. Additionally, a concentrated bed of sand grains was observed near the column after a dilution of 20%. While diluting the sludge improved the concentration of sand and heavy Fe minerals, it did not induce vivianite concentration.

The costs for a magnetic separator are directly related to its required capacity. The spiral yielded 40-50% of sludge to the product, meaning that the capacity and costs for the magnetic separator would be reduced with 50-60%. Before spiral pre-concentration can be applied, adjustments are needed to increase the vivianite recovery, such as changing the shape and slope of the spiral. If this is succeeded, vivianite recovery plants could produce a vivianite concentrate which can be used for fertilizer production, pigment for paint or for lithium-ion battery production.



# **Contents**

Ack	knowledgements	iii		
Abs	stract	٧		
List	t of Figures	ix		
List	t of Tables	X		
Non	lomenclature x			
1 1 1 1	Introduction  1.1 Problem statement	1 1 1 2 2 3		
2	Literature Review  2.1 Phosphates 2.1.1 Phosphate scarcity 2.1.2 Phosphate removal from wastewater 2.1.3 Phosphate recovery 2.1.4 Vivianite recovery 2.1.5 Sewage sludge characteristics  2.2 Spiral density concentration 2.2.1 Forces on particles in spiral concentrators 2.2.2 Force balance diagram. 2.2.3 Spiral concentration with sewage sludge	6 7 8 9 10 11		
3	Material and Methods 3.1 Material selection 3.1.1 Viscosity measurements 3.1.2 Synthetic and sewage sludge 3.2 Centrifugal experiment 3.2.1 Definitions 3.2.2 Theory 3.2.3 Dimensions 3.2.4 Sample analysis 3.5 Spiral concentration experiments 3.3.1 Definitions 3.3.2 Dimensions 3.3.3 Spiral testing	20 21 21 22 23 24 24 24		
4	Results  4.1 Centrifugal experiment	29		

		4.3.1 Solids and elemental analysis	32
		4.3.2 Influence of repulper	
	4.4	Spiral concentration with diluted sewage sludge	34
		1.4.1 Solids and elemental analysis	35
		1.4.2 Spiral performance	37
5	Disc	ession	39
	5.1	Measurement accuracy	39
	5.2	Centrifuge limitations and possible improvements	
		Spiral concentration for vivianite recovery	
		5.3.1 Synthetic sludge	41
		5.3.2 Digested sewage sludge	41
		5.3.3 Effect of diluting sewage sludge	43
	5.4	Financial analysis	44
6	Con	lusion	47
7	Rec	mmendations	49
Bi	bliog	aphy	50
Ar	pend	x	54
r	A	·· Fables and figures	_
	В		55

# **List of Figures**

2.1	Sustainable phosphorus supply and demand measures for meeting long-term future global food demand.[8]	6
2.2 2.3	Molar Fe:P ratio and % of total phosphorus bound in vivianite in digested sludge[62] Proposed process for wastewater treatment and P recovery, edited from Wilfert et al.	7
2.4	2017[61]	8
2. <del>4</del> 2.5	Image of a spiral concentrator[12]	9
2.6	Secondary flow on a spiral trough.[20]	11
2.7	Schematic drawing of a spiral and its trough.[27]	12
2.8	Forces acting on a particle flowing on a spiral trough.[27]	12
2.9	Particle-particle interactions in fluid transport[4]. With $\tau_{zz}$ being the dispersive stress,	12
2.0	and $\tau_{xz}$ the shear stress	14
2.10	Force balance diagram for particle motion on a spiral trough	15
	Spiral performance on Australian silica sand with Heavy Minerals (HM), organic mate-	. •
	rial and ultra-fine particles (-75 $\mu$ m)[40]	17
2.4	Dhaansana far tug agusana aludan agusalag with different temperaturas	20
3.1	Rheograms for two sewage sludge samples with different temperatures	20
3.2	Schematic cross-section of the centrifuge	22
3.3 3.4	Diagram of the centrifuge setup.	23
3. <del>4</del> 3.5	The centrifuge setup at the start of an experiment.	23 24
3.6	Spiral trough and splitter ranges L1 & L2	25
		20
4.1	Volatile and non-volatile solids content of the feed, product and tailings samples per	<b>~</b> =
	centrifuge splitter distance. Data labels indicating the fraction of solids.	27
4.2	Theoretical vivianite recoveries for different particle sizes	28
4.3	Particle size distributions of sand in the product for three different feed rates	29
4.4	Sand and PET recovery curves for three different feed rates	31
4.5 4.6	Sand enrichment for three different feed rates	31 31
4.0 4.7	Volatile solids and non-volatile solids contents of the product, middlings and tailings	31
<b>⊣.</b> /	samples for three different spiral feed rates. Data labels indicating the fraction of solids.	33
4.8	Volatile and non-volatile solids contents of the product, middlings and tailings samples	00
1.0	taken from the third turn of the spiral. Feed rate of 1.4 kg/s	34
4.9	Image of the repulper, red arrows indication how the flow is redirected	34
	Viscosity curves for diluted sewage sludge	35
	Volatile and non-volatile solids contents of the product, middlings and tailings samples	
	for undiluted and diluted sludge. Data labels indicating the fraction of solids. Feed rate	
	of 0.8 kg/s	36
4.12	Non-VS recovery plotted against sludge yield for different diluted sludge mixtures. Feed	
	rates around 0.8 kg/s	37
4.13	Spiral efficiency for undiluted and diluted sludge mixtures. Feed rates around 0.8 kg/s.	38
5.1	Synthetic sludge (A) and sewage sludge (B) entering the spiral. Red circles indicate	
	the different flow behaviours.	41
۸ 4		
A.1	Viscosity curves for synthetic and sewage sludge	55 55
B.1	Connection of cylinder to drill with two plates	ບວ

B.2	The closed-loop spiral setup.	56
B.3	Photos of the splitter configurations	56
B.4	A: Sludge flow before the repulper covering 90% of the trough. B: Sludge flow after the	
	repulper covering 80% of the trough	57
B.5	Slow-moving bed of sand near the column in 20% diluted sludge	57
B.6	Map of the Netherlands showing all sewage treatment plant locations[52]	58

# **List of Tables**

	3 3 4 4 4 4 4 4 4 4 4 4 4 4 4 4 4 4 4 4	28
4.2	Results from the spiral experiment with synthetic sludge, 10-200 µm sand particles &	
	1 mm PET flakes	30
4.3	Results from solids and elemental analysis of the spiral experiment with sewage sludge.	32
4.4	TS, VS and Fe and P concentrations for diluted and undiluted feed samples	35
4.5	Results from solids and elemental analysis of the spiral experiment with diluted sewage	
	sludge. Feed rate of 0.8 kg/s	36
5.1	Results of spiral experiments with undiluted sludge, with and without the repulper. Feed	
	rates of 0.9 kg/s	42
5.2	Costs for a SLon magnetic separator[38, 48] and a Multotec MX7 spiral	44
A.1	Centrifugal experiment: TS and VS content of samples taken in triplicate from the feed,	
		54
A.2	Centrifugal experiment: TS and VS content of samples taken without centrifuging and	
	while centrifuging, without splitting. Including Fe and P content determined by ICP-OES	
	analysis	54

# **Nomenclature**

#### **Abbreviations**

Anammox Anaerobic ammonium oxidation **CPR** Chemical phosphorus removal

ds Dry solids

**EBPR** Enhanced biological phosphorus removal

FePs Iron phosphates

**ICP-OES** Inductively coupled plasma optical emission spectrometry

non-VS Non volatile solids o-P ortho-Phosphate

PAH Polycyclic aromatic hydrocarbons

PET Polyethylene terephthalate **STP** Sewage treatment plant

TS Total solids VS Volatile solids **XRD** X-ray diffraction **XRF** X-ray fluorescence ZFL Zero force line **ZFS** Zero force surface

#### **Greek Symbols**

α

Primary slope Fluid viscosity  $kg/m \cdot s$ η λ Linear concentration Angular velocity rad/s ω Constant of proportionality (Equation 2.7) φ

 $kg/m^3$ Fluid pulp density  $\rho_f$  $kg/m^3$ Particle density  $\rho_p$ Stress Рa τ Trough slope θ

#### **Roman Symbols**

С Volume concentration of solids  $C_0$ Maximum possible volume concentration of solids Maximum trough depth  $c_y$ mSettling cut-size  $\mathsf{d}_h$ mParticle diameter  $\mathsf{D}_n$ m Radial cut-size  $d_r$ m  $F_b$ Bagnold force Ν

$F_{C}$	Centrifugal force	N
$F_d$	Drag force	N
$F_f$	Friction force	N
$F_g$	Gravitational force	N
$F_i$	Inward secondary gravitational force	N
$F_N$	Normal component of all forces	N
g	Gravitational constant	$m/s^2$
h	Flow depth	m
$k_1$	Proportionality constant (Equation 2.8)	
N	Ratio of inertial stress to viscous stress	
$P_{\mathcal{Y}}$	Dispersive pressure	Ра
r	Radial distance	m
$r_i$	Inner radius	m
$r_o$	Outer radius	m
u	Pitch height	m
V	Volume	$m^3$
V	Primary fluid velocity	m/s
$v_p$	Particle velocity	m/s
$v_r$	Radial fluid velocity	m/s
$v_{v}$	Vertical fluid velocity	m/s
$v_{eq}$	Equilibrium velocity	m/s

# 1 Introduction

Phosphate is slowly becoming a scarce resource worldwide. In worst-case scenarios, 40-60% of all phosphate resources will be extracted by 2100[55]. Phosphates are used in fertilizers for our food production and therefore are of great importance to mankind, especially because alternatives are not yet available. Because of its future scarcity, recycling of phosphates will become a necessity in the long term. One promising secondary phosphate resource is wastewater. Wastewater treatment plants currently remove phosphorus to prevent eutrophication in surface waters. This collected phosphorus is then either burned or recycled with low-efficiency techniques. This thesis focuses on innovative technology for improved phosphate recovery from wastewater.

#### 1.1 Problem statement

While the water processing industry has focused mainly on the mineral struvite for phosphorus recovery from wastewater, a recent study proved that the ferro-phosphate mineral vivianite is the most stable phosphate mineral in anaerobically digested sewage sludge, and has the highest recovery potential. A technique has been developed to precipitate vivianite in sewage treatment plants by adding iron, and then recover these minerals from the sludge using a magnetic separator. This process has is called Vivimag and shows high recovery potential, as almost all of the phosphorus in the wastewater precipitates as vivianite[61]. Although magnetic separation works well, the processing costs are relatively high. As long as vivianite recovery is more expensive than the conventional phosphorus recovery methods, sewage treatment plants will most likely not prefer this new technique, unless regulations prescribe elevated recovery levels.

# 1.2 Proposed solution

To reduce the processing costs for vivianite recovery, an inexpensive pre-concentration step could be introduced which recovers vivianite minerals by density concentration, as vivianite minerals have a higher density than other components in digested sewage sludge. A wide variety of concentration tools based on density differences exists. As digested sewage sludge has a relatively high viscosity, particle migration velocities are limited, and therefore a concentrator with a small fluid thickness is desired. The used density concentrator in this study is the spiral concentrator, where the fluid film is generally only millimeters thick. Spirals are relatively cheap and easy tools and can handle high capacities. A spiral can possibly be used as a pre-concentration step before magnetic separation, decreasing the capacity for the magnetic separator and thereby reducing its processing costs. Spiral concentration is mainly used in the mining industry, where the processed materials are slurries of water and ores or coals. Spirals have never been applied for processing viscous fluids such as sewage sludge, and therefore the feasibility of this is researched in this thesis.

# 1.3 Research questions

The goal of this study is to investigate the feasibility of vivianite recovery by spiral concentration, to reduce the cost of vivianite extraction from sewage sludge. The main research question is defined as follows:

Can spiral concentration be used for concentration of vivianite in digested sewage sludge?

With the following sub-questions:

1.4. Hypothesis 2

- (i) Which factors influence the separation of particles on spiral concentrators?
- (ii) Which forces are required to concentrate vivianite minerals in sewage sludge, and how can these be achieved on a spiral concentrator?
- (iii) Which vivianite recoveries and grades can be achieved by spiral concentration of sewage sludge?
- (iv) What is the financial benefit of using spiral concentration as a pre-concentration step for vivianite recovery?

# 1.4 Hypothesis

It is expected that spiral concentration will work to some extent on digested sewage sludge. However, it is uncertain how effective the recovery of vivianite minerals will be, as spiral concentration has never been performed on fluids with similar characteristics as sewage sludge. The effect of the viscosity of the sludge and the presence of organic fibers on the effectiveness of the separation is uncertain, as spirals are normally used for ores and coals suspended in water, and only for these materials literature and results are available.

Some slightly related works have been found[14, 40, 41], where organic material was effectively removed from the desired product using spirals. Next to that, Jain and Rayasam[26] showed that small and dense particles are more likely to settle, while larger and lighter particles will move upwards and towards the outer rim of the spiral, as shown by Equation 2.15 and 2.16 in Section 2.2.1. It is expected that solids will concentrate on the inner flow, but migration velocities will be limited due to the high viscosity of sewage sludge. The grade of the product will most likely be relatively low, as the upwards and outwards movement of the fluid is limited because of its high viscosity, meaning that the outwards movement of organic particles is limited too. Because spirals have never been used to treat sewage sludge, and the exact behaviour of sludge on spirals cannot be modelled accurately, lab experiments are performed.

# 1.5 Scope of work

The following tasks are performed during this research:

- A literature study on phosphate scarcity and phosphate recovery in sewage treatment plants.
- A literature study on the separation mechanism on spiral concentrators, and previously performed experiments with material characteristics similar to the materials in sewage sludge.
- Computation of forces acting on a spiral to predict the behaviour of particles in sewage sludge.
- Viscosity measurements on sewage sludge.
- Production of a synthetic sludge with similar characteristics as sewage sludge. This will be used for the first tests, as it is more stable and retains its quality throughout the tests.
- Design of a centrifuge test set-up to investigate particle migrations through sewage sludge.
- Perform experiments with the test set-up and determine its efficiency.
- Set up a closed-loop spiral circuit to enable testing.
- Test the spiral concentrator with synthetic sludge with multiple feed rates and splitter positions and analyse the samples.<sup>1</sup>

<sup>&</sup>lt;sup>1</sup>Performed by S. de Graaf as part of his BSc thesis

- Test the spiral concentrator with digested sewage sludge with multiple feed rates and splitter positions and analyse the samples.
- Calculations of the financial benefit of using spiral concentration as a pre-concentration step for vivianite recovery from digested sewage sludge.

The following tasks are out of scope for this research:

- Determination of the exact vivianite concentration in sewage sludge. As phosphorus can be
  partially bound to other metals, vivianite can have impurities and can be amorphous, it is difficult
  to determine the exact vivianite concentration. In this study, the elemental composition will be
  used to approximate the vivianite concentration.
- Modelling of fluid and particle flow on the spiral.

# 1.6 Structure of report

The structure of this report is based on the different stages of the research. Firstly, a literature study was done on phosphate in wastewater and spiral concentrators, given in Chapter 2. The theory of spiral concentration is described, and also relevant studies with spirals are summarized. Chapter 3 describes the experimental procedures and laboratory tests that were performed. Firstly the used materials are described, followed by descriptions of the two different experimental setups that were designed and tested; a centrifugal and a spiral experiment. The results of these experiments are shown and analyzed in Chapter 4. Chapter 5 discusses these results. Also the financial benefit of pre-concentration of vivianite is given in this chapter. The conclusion of this research is given in Chapter 6, and finally in Chapter 7 recommendations for further research are given.

# 2 Literature Review

This chapter describes the future phosphate scarcity and the importance of sewage sludge as a secondary phosphate resource. Furthermore, it is described how phosphate minerals are formed in sewage sludge, and how these can be recovered through different separation techniques.

# 2.1 Phosphates

This section discusses the importance of phosphates in our daily lives, and the importance of recovering it from sewage sludge. Next to that, the mineral formation in sewage treatment plants (STPs) is described.

# 2.1.1 Phosphate scarcity

Phosphorus (P) is a crucial element for all life. On earth, phosphorus mainly occurs as various types of phosphates ( $PO_4^{3-}$ ), due to the earth's oxygen atmosphere and the instability of elemental phosphorus. Phosphate is a building block for molecules, acting as a sophisticated glue in DNA, in energy transfer molecules or in molecules that are part of cell membranes[57]. Furthermore, calcium phosphate minerals are part of skeletal structures or teeth of many organisms[5, 17]. Phosphate can exist in organic molecules, as polyphosphates or bound to metals, occurring both soluble and insoluble. Free dissolved inorganic phosphate is called ortho-phosphate (o-P)[58].

A sufficient phosphorus supply is important for both plants and animals. The daily consumption of a growing crop ranges from 0.1-2 kg per hectare. For cattle, the daily consumption ranges from 0.2-0.9 g (chicken) to 45-85 g (cow)[42]. Animals obtain phosphorus from food, while plants take it from the soil. Before the existence of fertilizers, crop production was stimulated by using manure from animals as a phosphorus source. Therefore most farmers had both crops and cattle, so that the manure of the cattle could be used for the crops. With the arrival of fertilizers, large scale crop production became possible, independent of the phosphate from manure. Livestock farming is nowadays generally concentrated in densely populated areas, while crop production is located in areas with a low population density. The majority of agriculture worldwide thereby has become dependent on phosphates from fertilizers[32].

Of all the mined phosphate rocks worldwide, around 80% is used for fertilizers, 10% for detergents, 5% in animal feeds and the remaining for other applications such as steel production, matches and water softeners[15]. The global production of phosphate fertilizers is expected to grow the next decades due to the world population growth and increase in wealth[55]. This production is extractive and non-renewable, therefore it would ultimately lead to depletion of high-grade P resources. The resources are unequally distributed across the globe; almost 60% is reported to be located in Africa. In worst-case scenarios, about 40-60% of the current resource base would be extracted by 2100[55]. This is problematic, as phosphate is a non-replaceable resource, there are currently no alternatives for phosphates. Therefore recycling of phosphates becomes more important, which is currently insignificantly done. The predicted phosphate demand, including sustainable demand and supply measures created by Cordell & White are visualized in Figure 2.1[8]. This research focuses on the reuse of human excreta.

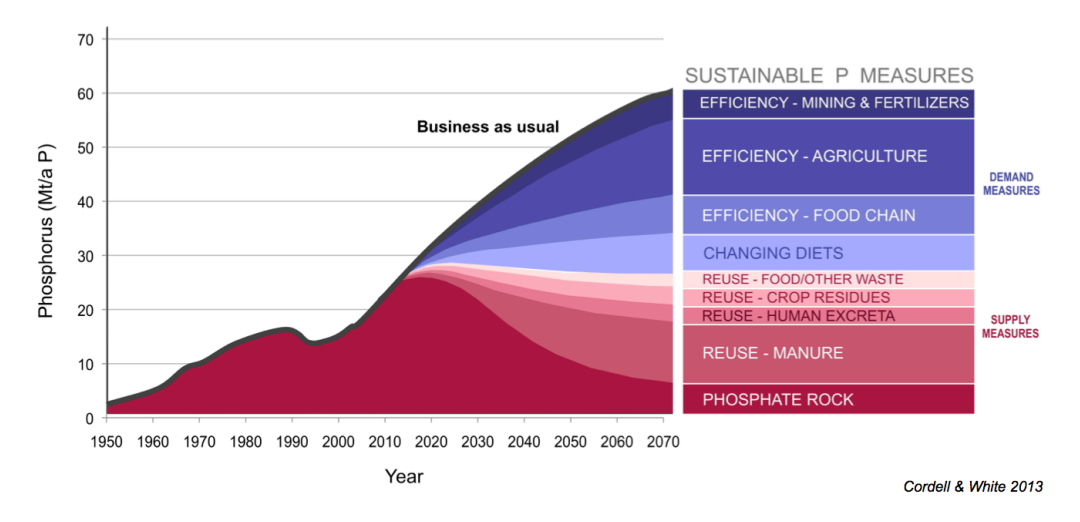


Figure 2.1: Sustainable phosphorus supply and demand measures for meeting long-term future global food demand.[8]

#### 2.1.2 Phosphate removal from wastewater

Phosphorus is present in human excreta, which ends up in our sewage systems. In STPs, this phosphorus is removed from wastewater to prevent eutrophication in surface waters, where the processed water is effused. Annually, about 1.3 Mt phosphorus is treated in STPs[55]. It is estimated that in Europe, 20-30% of the fertilizer demand can be met by using the phosphorus that ends up in sludge in European STPs[43], which is approximately 370 kton[51]. The two most used phosphorus removal techniques are enhanced biological phosphorus removal (EBPR) and chemical phosphorus removal (CPR) using iron or aluminium salts[59]. CPR is more widely used, usually with iron salts, as they are cheaper than aluminium salts. Iron is also used in EBPR plants to support phosphorus removal, but also to prevent hydrogen sulphide emissions during digestion and it works as a coagulant to improve sludge dewatering[59]. It can also be present as a natural component in the influent of the STPs.

In EBPR plants, magnesium is added to the sewage water and pH is increased to generate struvite, MgNH $_3$ PO $_4 \cdot 6$  H $_2$ O[9]. The precipitation and recovery of struvite can be performed directly in the sludge, or in the reject water after sewage sludge dewatering[59]. There are multiple techniques for struvite precipitation, but the market share is limited as they can only be used in combination with EBPR, while CPR methods are more dominant. CPR has lower investment costs, and the processes are easier to control. Furthermore, the energy requirements for EBPR are slightly higher, and sludge dewatering is more difficult than in CPR. The phosphate recoveries for struvite precipitation techniques are relatively low; 10-40% of the influent phosphate can be recovered[58]. The potential is low too, as part of the phosphate is bound to compounds with lower solubility than struvite, such as aluminium or iron phosphates[62].

For CPR, iron is added to sewage water by dosing iron salts or coagulants. The iron then precipitates as different iron phosphate minerals (FePs). One of these minerals is vivianite, Fe(II) $_3$ [PO $_4$ ] $_2 \cdot 8$  H $_2$ O. It forms in absence of oxygen in non-sulphidic systems and is stable over a broad pH range. Vivianite can form directly upon Fe(II) dosing, or when Fe(III) is reduced to Fe(II). It is believed that during anaerobic digestion, all Fe(III) is reduced to Fe(II), so it is irrelevant which iron ion is mixed with the sludge. The chemical reaction is shown below (Equation 2.1). The sulphate supply is limited in digesters, so insoluble sulphide compounds will not hinder the vivianite formation. Therefore anaerobic digesters offer optimal conditions for vivianite formation[31]. P. Wilfert discovered that for digested sludge with high iron contents (molar Fe:P = 2.5), 70-90% of all phosphate was bound in vivianite. Figure 2.2 shows how much phosphorus in digested sludge is bound in vivianite for different Fe:P ratios. Wilfert concluded that vivianite was the main iron phosphate phase in sewage sludge[58]. Vivianite

can induce higher phosphate recoveries than struvite, as vivianite has a relatively low solubility. In STPs, vivianite formation naturally takes place as iron ions are always present, and as has been noted before, CPR with iron salts is worldwide the most common phosphate removal technique. Therefore a phosphate recovery technique using high iron dosing in CPR could lead to a higher recovery efficiency compared to routes relying on struvite.

$$OrganicP - > PO_4^{3-}$$

$$Fe(OH)_3 + 3H^+ + e^- \longrightarrow Fe^{2+} + 3H_2O \qquad (2.1)$$

$$3Fe^{2+} + 2PO_4^{3-} + 8H_2O \longrightarrow Fe_3(PO_4)_2 \cdot 8H_2O$$

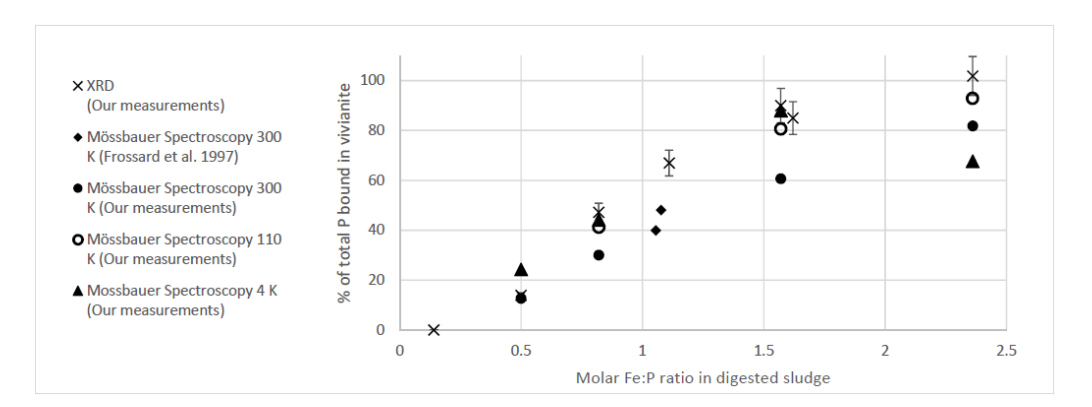


Figure 2.2: Molar Fe:P ratio and % of total phosphorus bound in vivianite in digested sludge[62].

# 2.1.3 Phosphate recovery

Currently, there are three P recovery methods from wastewater. Firstly, sludge can have agricultural usage. Sludge is cleaned, and can then directly be applied on agricultural land. This is a low-cost option for local P recycling that is widely used; 50% of all sludge in the USA was used for agriculture in 2004[34], and 40% of all sludge in the 27 EU countries in 2005[29]. There are public concerns about heavy metals and other pollutants that might be present in the sludge. Another disadvantage of this recycling option is that there are areas where already a surplus of P exists because of manure surpluses. Transporting the sludge from these areas is problematic because of the costs and logistics involved. A pure high-value P product that can be transported is preferred over a mixed product like sludge[59].

One method to produce a high-value P recovery product is by struvite precipitation. As has been mentioned before, the recovery efficiencies are limited, and it can only be recovered in combination with EBPR and sludge digestion, and ideally with a P stripping process[9]. Sludge is also incinerated in several countries[29]. Phosphorus is recovered from the ashes of these mono-incinerators. P is then present in a concentrated form, and nearly all of it can be recovered. However, recovery of P alone is not a sufficient economic basis to build sludge incinerators, and the recovery techniques demand expensive infrastructure for incineration[59].

Iron could play a more important role in future STPs. By adding Fe, STPs can become energy and P factories. Energy-producing STPs already exist[37]. Figure 2.3 shows a proposed process for such an energy- and phosphorus producing STP. Sewage water with high nitrogen and phosphorus concentration is first processed by adding Fe for coagulation and P removal. The remaining nitrogenrich wastewater is then processed by anaerobic ammonium oxidation (anammox), resulting in a low P and N content effluent. The separated sludge is anaerobically digested, which produces biogas. After sludge digestion, P will be recovered from the FeP-rich sludge. Ideally, one would separate the FePs into pure Fe and P, so that the iron can be re-used in the process, and P can be sold. Wilfert

tried this by adding sulphides to the sludge, but the released phosphate quickly formed precipitates again with other elements in the sludge or bound to other inorganic phases in the sludge solids, and therefore the phosphates could not occur as free dissolved molecules for a long time[62]. Therefore a separation technique that separates vivianite minerals from the sludge seems most logical. Once vivianite is separated, it can be directly used to produce valuable products. It can also be dissolved with KOH at alkaline pH of about 12[58]. Vivianite then separates into  $K_3PO_4$ , which can be used for fertilizers, and  $Fe(OH)_2$ , that can be re-used for vivianite precipitation in the aeration tank. The vivianite separation techniques, by magnetic or density concentration, are described in the following sections.

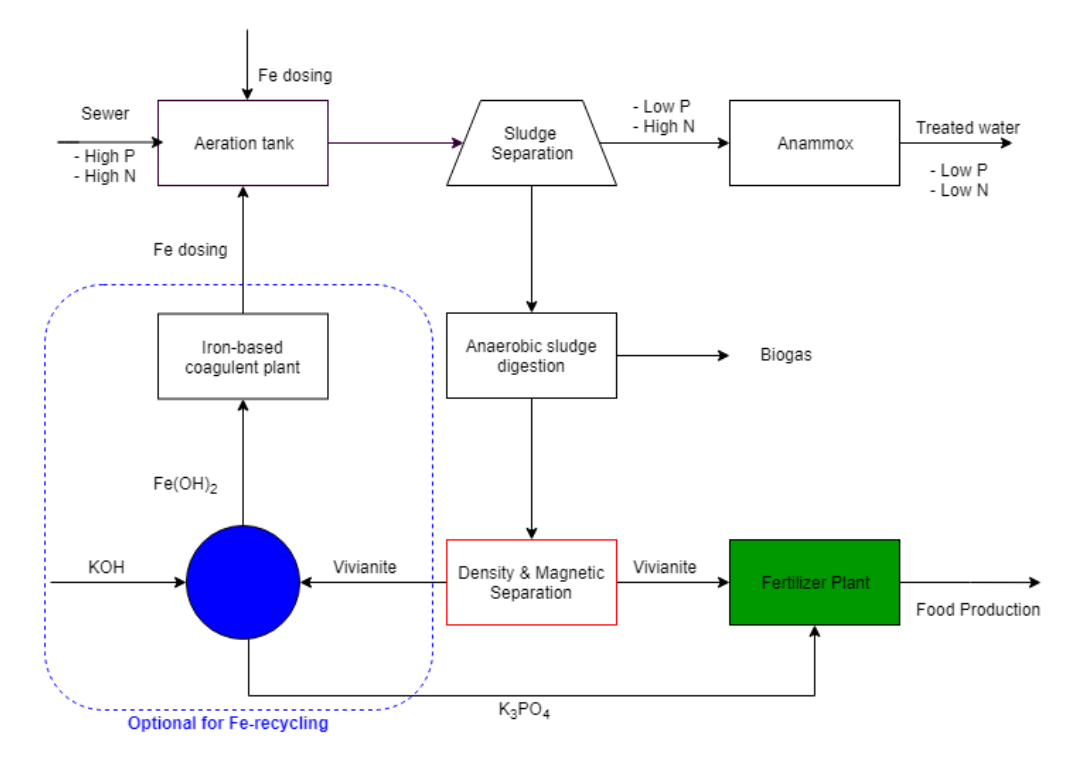


Figure 2.3: Proposed process for wastewater treatment and P recovery, edited from Wilfert et al. 2017[61].

#### 2.1.4 Vivianite recovery

Different techniques are possible for the recovery of vivianite from sludge. The separation techniques are based on property differences between the vivianite minerals and the other particles present in the sludge. There are, however, limitations in the available options. Due to the high viscosity in sewage sludge, the drag on vivianite particles is large, and therefore the velocity at which vivianite can move through the sludge is relatively low. That is why separation techniques are favored where vivianite particles are separated over a small distance. This reduces the necessary residence time for an efficient separation.

Vivianite occurs as small (10-200 µm) crystals or aggregates in digested sewage sludge[13, 62]. Pure vivianite is white transparent but oxidizes when exposed to air, resulting in a blue color. At room temperature, Fe(II) reduces to Fe(III), making the mineral amorphous which is called meta-vivianite. Wilfert et al. showed that in vivianite with impurities, such as magnesium and calcium, 89% of all Fe(II) was oxidized within 48 hours[62]. Vivianite minerals are paramagnetic, enabling them to be separated by magnetic separators. This has been done before by Seitz et al. for easier identification of vivianite using X-ray diffraction (XRD)[44]. Wilfert et al. used a magnetic Jones separator for wet separation. Dry separation using a Frantz separator was not possible, as sludge drying could lead to vivianite particles being covered in an organic matrix[61]. The Jones separator is a wet high-intensity separator. Sludge flows through the separator by pipes into plate boxes. These plate boxes are

grooved so that the magnetic field is concentrated at tips of the ridges. Magnetic particles are held by the plates, while nonmagnetic sludge passes through the plate boxes[25]. After separation, non-magnetic particles that are stuck between the plates are removed. After that, magnetic particles are flushed away and captured.

Wilfert et al. tested the Jones separator on two digested sludge samples. Recoveries between 40-60% were found. The iron and phosphate content of the separated material could be double or triple the content of the initial sludge[61]. The separated fractions had a vivianite grade of 52-62%, the rest being volatile solids (20%), less than 10% quartz and a small quantity of pyrite and siderite [39]. Volatile solids are substances that can easily transform from solid to vapor and can be ignited or burned. This high volatile solid content could be explained by the presence of organic compounds, or other compounds that lose crystal water during heating, such as carbonates but also vivianite[61].

Even though magnetic separation of vivianite has shown high potential, the processing costs are relatively high. Therefore a cheaper mechanism will be investigated; density concentration. Vivianite has a significantly higher density (2.65 g/cm³) than the organic material (around 1.3 g/cm³) in sewage sludge, and therefore density concentration could be an option. Particle migration velocities through sludge are relatively low due to the high viscosity and the organic matrix, therefore particles should only need to migrate over a small distance to reduce residence times. Thin stream concentrators provide this small fluid thickness and therefore seem to be the most suitable. For this research, the spiral density concentrator is used. The spiral concentrator can possibly be used as a pre-concentration step to reduce the required capacity of the magnetic separator. This would be beneficial, as spirals are significantly cheaper and can handle high capacities, and it would reduce the required capacities for the magnetic separator. Spirals are also easy to operate and require limited maintenance.

#### 2.1.5 Sewage sludge characteristics

Digested sewage sludge is a complex heterogeneous mixture. The primary components in sludge are mineral grains from soil and industrial sources, and organic residues including plant detritus, hairs, plastics, and pigments. The secondary components consist of inorganic precipitates, released during anaerobic digestion, and an organic matrix. This organic matrix contains amorphous degraded organic matter, digester biomass, and microbial detritus[33]. The mineral grains are mainly quartz particles, and the vivianite particles are part of the inorganic precipitates. A microscopic image of vivianite particles in dried digested sludge is shown in Figure 2.4. It shows that vivianite minerals are present in an organic matrix, their blue color is caused by oxidation. Frossard et al. also noticed the presence of small vivianite particles embedded in an organic matrix using XRD[13]. The total solids (TS) and volatile solids (VS) content of digested sewage sludge from the Nieuwveer STP, which is the sludge used in this research, have previously been measured to be 41.6 g/kg and 24.8 g/kg respectively[60], so here the organic matter contributed to 59% of the total solids.

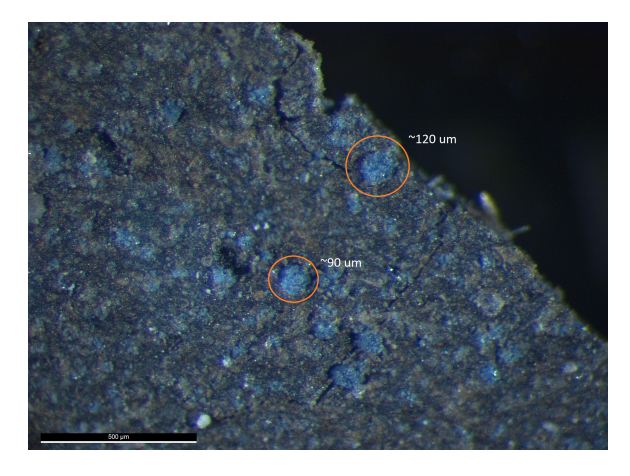


Figure 2.4: Microscopic image of dried digested sewage sludge showing vivianite minerals.

# 2.2 Spiral density concentration

Spiral concentrators are widely applied in mineral processing, but most extensively in heavy mineral sand deposits and fine coal recovery[63]. The concentrator is a helical conduit of a semi-circular cross-section, visualized in Figure 2.5. As slurry flows spirally downward, particles stratify due to centrifugal forces, combined with differential settling rates and the effect of interstitial trickling through the flowing particle bed[63]. The centrifugal force tends to move particles to the outer rim. Because of the shape of the trough, particles then move inward towards the bottom of the trough. Heavy particles settle out of suspension and flow down the spiral closer to the center. There they experience less centrifugal acceleration. The lighter particles move closer to the free surface, and are carried to the outer rim due to centrifugal acceleration.

At the bottom of the spiral, the heavy particle- and light particle concentrated fluids are separated with a splitter. This splitter is adjustable. Alternatively, holes at the center of the trough can be used to remove the heavy particles[47]. Steeper spirals handle higher capacities, produce higher grades but have low recoveries. Shallow slopes are more suitable for feed with small specific gravity differences and fine particle sizes[46]. Capacity can also be increased by using a double start spiral concentrator, here two spirals are wound around a single column, thereby doubling the capacity.

The fluid flow on spirals consists of two components; a primary (down trough) flow, with a secondary transverse circulation superimposed. This secondary flow arises from greater frictional retardation on the lower layers of the primary flow compared with the upper layers[20]. While the primary flow moves around a bend, the top layers experience greater inertia or centrifugal force than the bottom layers, and therefore move outward, and push the bottom layers inward[16]. Figure 2.6 shows the movement of secondary flow on a spiral trough.

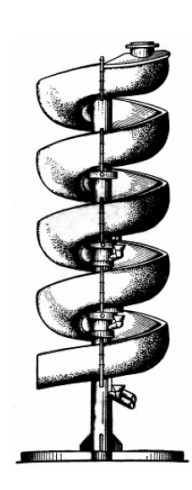


Figure 2.5: Image of a spiral concentrator[12].

The spiral trough can conceptually be divided into two main zones, separated by a transition zone, with all three zones exhibiting different aspects of the fluid flow. In the inner zone, near the column, a slow-moving bed of particles is created, overlaid by a free motion region controlled by the secondary flow. A rising component of this flow lifts lighter particles into the upper levels of the flow, moving them back into circulation[20].

The outer zone of the trough, near the rim, can be considered a recovery zone, as particles settle into lower levels to be transported inwards again to the inner zone. Behaviour in this zone is regulated by the primary flow velocity and will control the quantity and composition of the recovered material in the inner zone[20].

The intermediate transportation zone exhibits a free motion above a bed region, being relatively less concentrated and more mobile than the inner zone. The majority of the material in this zone moves with the secondary flow, so it can be seen as a transportation system, rather than a major separation factor. If the bed in this zone builds up to the point where it occupies most of the flow depth, the nature of the flow changes visibly. Then the secondary circulation is reduced and additional forces come into play, changing the separation in a predominantly bed-controlled mechanism[20]. This is generally undesired in spiral concentrators, as the secondary flow is of major importance for effective density concentration.

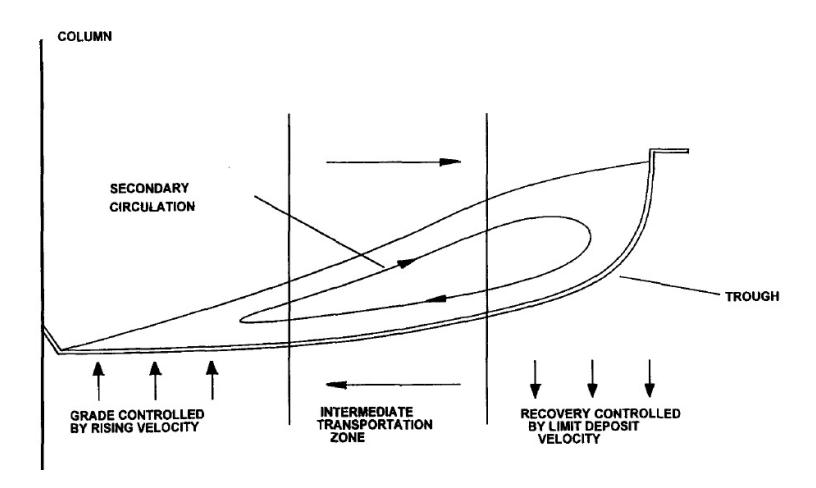


Figure 2.6: Secondary flow on a spiral trough.[20]

As the upper flowing layers in the secondary flow move in an outward direction, and the lower flowing layers in an inwards direction, there must exist a layer in between that neither moves inwards nor outwards. This is called the zero force line (ZFL), or in three dimensions, the zero force surface (ZFS). An equilibrium velocity exists on this surface, that causes the centrifugal (outward) force and gravitational (inward) force to be in equilibrium. Above the ZFS fluid moves outwards, and below it fluid moves inwards towards the column. The secondary circulation depends on the solid concentration and flow rate of the fluid. The optimum flow rate is where all particles are in suspension, and complete separation of particles is possible. This optimum depends on the solids concentration and has to be determined experimentally[26]. The solid concentration can reach a maximum, where beyond this maximum the secondary circulation will stop due to increased viscosity and shear rate. The ZFS will also vary with solid concentrations. Generally, the ZFS depth increases with an increasing solid concentration, due to increased viscosity and decreased fluid velocity[26].

In 1945, Gleeson[16] predicted that the secondary flow in spirals can lift low density particles to the top layer, move them outward and carry them to the low density tailing zone near the rim of the trough. The high density particles then settle in the bottom layer and move inward with the flowing fluid in direction of the column, so that heavy minerals are concentrated from the outer zone towards the inner zone. At the end of this chapter it will be shown that indeed, lighter and also larger particles are more prone to move the upper flowing layers, and then move outwards to the rim of the trough (Equation 2.15 and 2.16). In sewage sludge, the vivianite particles are generally smaller and of a higher density than the volatile organic solids. Ideally, all vivianite minerals would end up in the inner zone during concentration, for an optimal vivianite recovery. The organic solids, on the other hand, should concentrate as much as possible in the outer zone, for an optimal grade of the vivianite product.

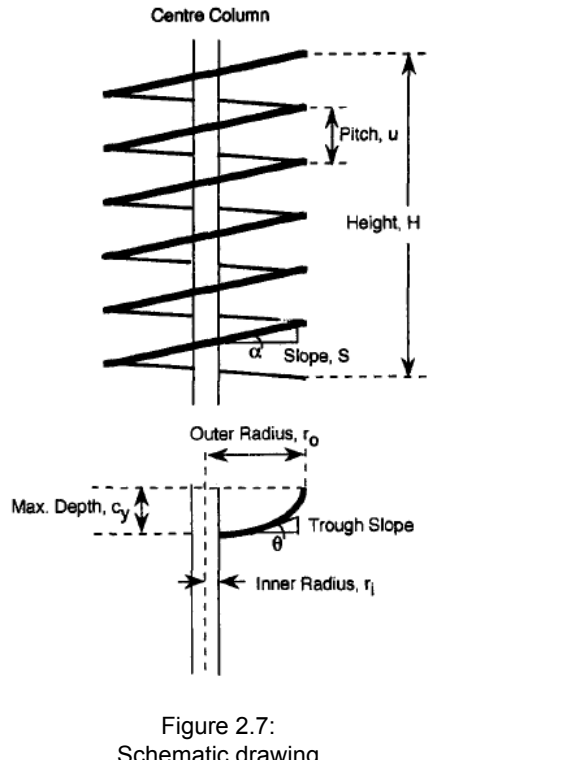
#### 2.2.1 Forces on particles in spiral concentrators

Spirals highly depend on their design parameters, such as diameter, number of turns, pitch, slope and the shape and dimensions of the trough. Calculations for the primary slope  $\alpha$  and trough slope  $\theta$  have been given in literature[27, 28]. The slopes at any point on the deck, at a radial distance r from the centerline are given as by the following equations:

$$tan(\alpha) = \frac{u}{2\pi r} \tag{2.2}$$

$$tan(\theta) = \frac{c_y}{r_o - r_i} tan \ arcsin \frac{r - r_i}{r_o - r_i}$$
 (2.3)

Where u is the pitch height,  $c_y$  the maximum trough depth, and  $r_i$  and  $r_o$  are the inner and outer radii of the trough from the centerline respectively, shown in Figure 2.7 and Figure 2.8.



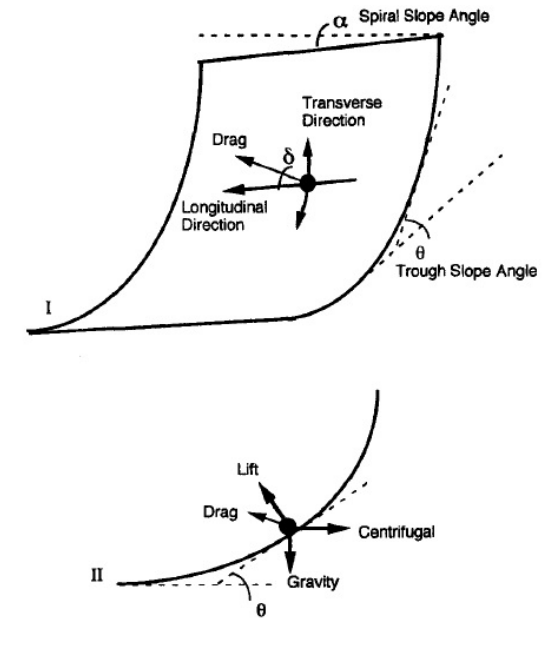


Figure 2.7: Schematic drawing of a spiral and its trough.[27]

Figure 2.8: Forces acting on a particle flowing on a spiral trough.[27]

Particles on spirals are subject to a medley of randomly fluctuating, transient and steady force fields, due to a mix of laminar, transitional and turbulent flow regimes. Generally, only rough estimates are possible for five principal forces: effective gravity, centrifugal, hydrodynamic drag, friction and lift forces[27], visualized in Figure 2.8. The gravity force  $F_g$  on a spherical particle of diameter  $D_p$  and density  $\rho_p$  in a fluid with a pulp density  $\rho_f$  is given by:

$$F_g = \frac{\pi}{6} D_p^3 g(\rho_p - \rho_f)$$
 (2.4)

Where g is the gravitational constant. The fluid pulp density  $\rho_f$  is dependent on the solids concentration. The centrifugal force  $F_C$  plays a significant role in spiral concentrators. For a particle moving with velocity  $v_p$  in a circular path with radius r,  $F_C$  is given by:

$$F_C = \frac{\pi}{6} \frac{D_p^3 v_p^2 (\rho_p - \rho_f)}{r} cos(\theta)$$
 (2.5)

Drag force in spiral concentrators is present as long as there is a velocity difference between the fluid and the particle. The direction is dependent on the relative motion of particle and fluid. This force is assumed to be the same as the drag exerted on a body in a flowing stream of fluid due to skin friction and eddies induced pressure difference between its upstream and downstream sides[1][26]. The drag force  $F_d$  is given by:

$$F_d = -\frac{\pi}{4} D_p^2 \rho_f ghsin(\alpha)$$
 (2.6)

Here, h is the depth of flow and the angle  $\alpha$  is the angle of the primary slope of the spiral.  $\rho_f gh$  is equal to the streamwise mean shear stress and  $\pi/4D_p^2$  is the particle surface area[1]. Resistance to motion of a particle on a spiral trough is proportional to the sum of all normal components of all forces  $F_N$  acting on that particle. The proportionality constant is the coefficient of dynamic friction under water  $tan(\phi)$ , which is according to Bagnold[4] virtually the same as the coefficient of static friction under water[27]. This leads to the following equation for the friction force  $F_f$ :

$$F_f = F_N tan(\phi) \tag{2.7}$$

Where  $tan(\phi) = 0.5$ , from Kapur & Meloy, 1998[27].

Hydrodynamic lift forces in spiral concentrators are often called Bagnold dispersive forces ( $F_B$ ), named after R.A. Bagnold, who first described these forces in 1954[4]. On spirals, the fluid in a film flowing under gravity has a velocity profile which increases with the height of the fluid. Particles in the fast flowing upper layer of the fluid collide with slower particles in the lower layer[11]. The force arises by influences of the nearby boundary, fluid shear, and the Magnus effect. The Bagnold force lifts the coarse, light particles into the high velocity layers. The balance between the Bagnold and gravitational force in a vertical column determines whether a particle lifts in upper layers or not[26]. An exact expression for the lift force still has not been determined, but an approximation has been given[27]:

$$F_b = k_1 F_d \tag{2.8}$$

Here constant of proportionality  $k_1$  varies from 1/7 to 1 [45]. It has been stated that "if a suspension of particles is subjected to continuous shear, then pressure tends to develop across the plane of shear at right angles to the surface of shear"[7]. Bagnold[4] proposed a factor N, the ratio of inertial stress to viscous stress:

$$N = \frac{\lambda^{\frac{1}{2}} \rho_p D_p^2}{\eta} \frac{du}{dy} \quad \text{for } \lambda < 12$$
 (2.9)

Here  $\lambda$  is the linear concentration given by:

$$\lambda = \frac{1}{\left(\frac{C_o}{C}\right)^{\frac{1}{3}} - 1} \quad \text{for } \lambda < 12 \tag{2.10}$$

 $\mathcal{C}_0$  is the maximum possible volume concentration of solids, 74% for spheres.

*C* is the volume concentration of solids.

 $\eta$  is the fluid viscosity.

 $\frac{du}{dy}$  is the mean rate of shearing.

For N>450, the inertia of the particle dominates its motion in the fluid, called the particle-inertia regime. For N<40, the viscosity of the fluid dictates the motion, called the macro-viscous regime. Between 40 and 450, a transition regime exists between inertia and viscosity dominance, under which dispersive pressure  $P_y$  exists between particles present in two layers in a fluid. Here particle interactions are a combination of collision and viscous motion. The interactions in the macro-viscous regime and particle-inertia regime are shown in Figure 2.9. The dispersive pressure in the transition regime is given by the following equation[4]:

$$P_y = 0.042(\lambda D_p)^2 \rho_p \left(\frac{du}{dy}\right)^2 \tag{2.11}$$

Jain and Rayasam[26] stated that since this pressure develops across the shear plane at right angles to the surface, the corresponding Bagnold force can be given by:

$$F_b = P_y \times \frac{\pi D_p^2}{4} \tag{2.12}$$

Now combining Equation 2.11 and 2.12 results in the final equation for Bagnold forces:

$$F_b = 0.033\lambda^2 D_p^4 \rho_p \left(\frac{du}{dy}\right)^2 \tag{2.13}$$

With Equation 2.13, the dominance of the Bagnold force over gravitational force on particle size and density can be shown, by taking the ratio of  $F_b$  over  $F_q$  (Equation 2.4):

$$\frac{F_b}{F_g} = \frac{KD_p \left(\frac{du}{dy}\right)^2}{1 - \frac{\rho_f}{\rho_p}} \tag{2.14}$$

Where K is a constant. For two particles with the same diameter  $D_p$  under identical flow regimes, but with different densities ( $\rho_+ > \rho_-$ ), Equation 2.14 can be written as follows:

$$\left(\frac{F_b}{F_g}\right)_{\rho_+} < \left(\frac{F_b}{F_g}\right)_{\rho_-} \tag{2.15}$$

This shows that a particle with a lower density  $(\rho_{-})$  will experience more lift than a particle with higher density  $(\rho_{+})$ . Similarly, two particles with the same density, but with different diameters  $(D_{+} > D_{-})$  under identical flow regimes can be written as:

$$\left(\frac{F_b}{F_g}\right)_{D_+} > \left(\frac{F_b}{F_g}\right)_{D_-}$$
(2.16)

Therefore, a large particle  $(D_+)$  will experience more lift than a smaller one  $(D_-)$ . Equation 2.15 and 2.16 show that particles will lower densities and larger diameters tend to experience more lift and will remain up in the fast flowing layers.

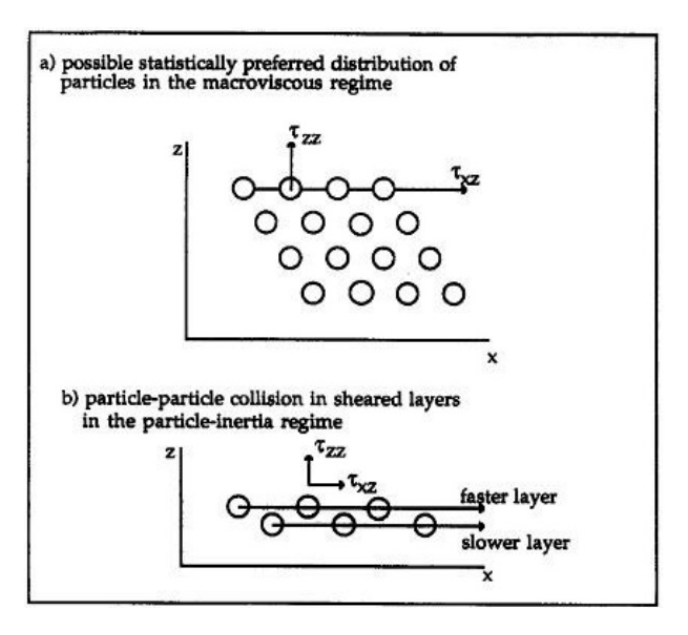


Figure 2.9: Particle-particle interactions in fluid transport[4]. With  $\tau_{zz}$  being the dispersive stress, and  $\tau_{xz}$  the shear stress.

#### 2.2.2 Force balance diagram

Particle motion on a spiral with an optimum flow rate can be explained by using a force balance diagram. Generally, particle motion will be in the same direction as the secondary flow: outwards above the ZFS, and inwards below it. Selective separation is governed by the balance between the Bagnold force and gravitational force on a particle. Frictional force and drag force play virtually no role in selective separation[26]. The gravitational force that is in the opposite direction of the Bagnold force, so perpendicular to the trough surface, is named  $F_q'$  and given by:

$$F_g' = \frac{\pi}{6} D_p^3 g(\rho_p - \rho_f) cos(\theta)$$
 (2.17)

The centrifugal force and primary and secondary components of the gravitational force do play a role in generating the secondary flow. The primary component relates to the primary flow and slope  $\alpha$ , and the secondary component to the trough slope  $\theta$ . The secondary component is directed inwards and will be called the inwards secondary gravitational force  $F_i$ , given by:

$$F_i = \frac{\pi}{6} D_p^3 g(\rho_p - \rho_f) sin(\theta)$$
 (2.18)

If  $F_c > F_i$ , the motion is outwards, and if  $F_c < F_i$ , motion is inwards. Similarly, if  $F_g' > F_b$ , particle motion is downwards, and if  $F_g' < F_b$ , particle motion is upwards. The diagram is shown in Figure 2.10.

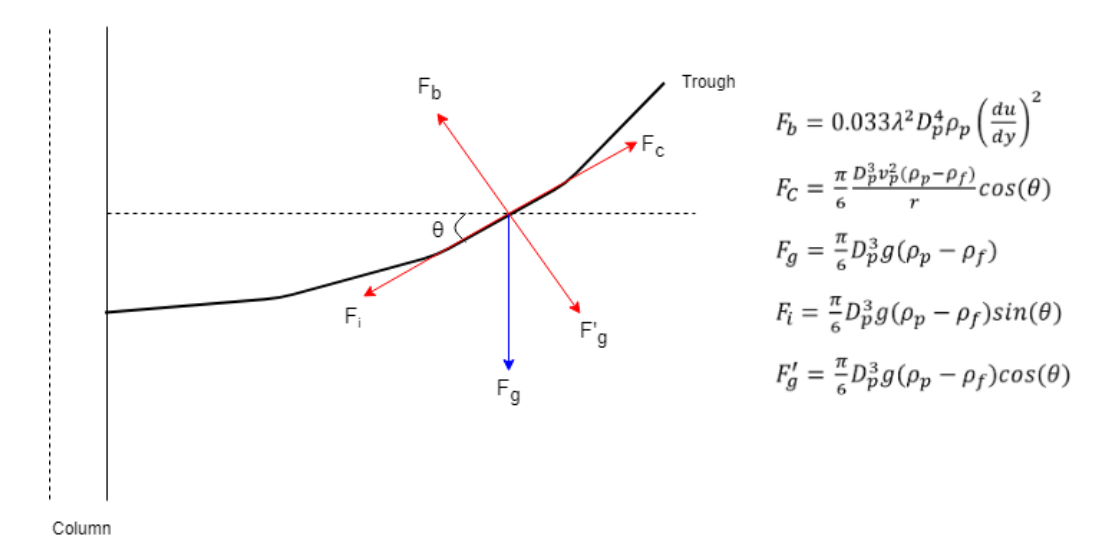


Figure 2.10: Force balance diagram for particle motion on a spiral trough.

For a radial force balance,  $F_i = F_C$ , the equilibrium velocity  $v_{eq}$  can be given by:

$$v_{eq} = \sqrt{r \cdot g \cdot tan(\theta)} \tag{2.19}$$

So the equilibrium velocity increases with radial distance from the column. With an exact velocity profile of a spiral, the ZFS can be determined using  $v_{eq}$ . As the primary flow velocity increases down the trough, the depth of the ZFS will change throughout the spiral.

The radial cut-size  $d_r$ , defining the minimal size of a particle to escape outwards driven by centrifugal force, opposing the liquid flow, is given by Holland-Batt[19]:

$$d_r = \left(\frac{18 * \eta * r * v_r}{(\rho_p - \rho_f)v^2 * (1 - C)^{4.6}}\right)^{0.5}$$
 (2.20)

With r being the radial position of the particle,  $v_r$  the radial velocity of the fluid, and v the primary velocity.

The vertical cut-size  $d_h$ , being the minimum diameter for a particle to settle under gravity, depends on the viscosity of the carrying fluid according to the following formula[19]:

$$d_h = \left(\frac{18 * \eta * v_v}{(\rho_p - \rho_f)g * (1 - C)^{4.6}}\right)^{0.5}$$
 (2.21)

With  $v_v$  being the vertical velocity component of the fluid velocity in cm/s, and the particle cut-size in  $\mu$ m. Equation 2.21 assumes spherical particles and a laminar fluid flow. The formula shows that for a higher viscosity  $\eta$  (in Poise), the cut-size  $d_h$  for a particle to settle under gravity will be larger. Or, with a higher fluid viscosity, smaller particles are more prone to move upwards with the vertical fluid

flow. Therefore, fine particle recovery is expected to decrease in the near column zone with increased viscosities.

Equation 2.21 gives a minimum particle size to settle under gravity, meaning all particles larger than this size *will settle*. However, it was previously shown in Equation 2.16 that larger particles will experience more lift than smaller ones. Here the cut-size is a minimum for particles to *move upwards*. This is because Jain & Rayasam[26] determined a Bagnold force equation proportional to the fourth power particle size, on contrary to the equation found by Burt[7], and later Atasoy and Spottiswood[3] and Kapur and Meloy[27, 28], where the equation was proportional to the second power of particle size.

Performance analysis of spirals has mainly been done empirically in the past decades. Several mathematical models are created to predict performance on spirals, but most of these models are fairly fundamental and have seen a limited application in the industry[53]. Furthermore, these models have not adequately explained the actual separation and secondary circulation, but primary flow equations have been derived with different considerations[26]. There is no consensus yet about the magnitude of the Bagnold force, but the most recent development has been the force balance diagram by Jain & Rayasam as shown in Figure 2.10. While this approach has not been validated by experiments, it does show the behavior of particles on a spiral trough and their selective separation.

#### 2.2.3 Spiral concentration with sewage sludge

Spirals are generally used for mineral and coal processing. The conventional spirals have a lower limit particle size of around 75  $\mu$ m. Fine heavy particles below this size are swept up in turbulent outer regions of the trough and are unable to migrate inwards towards the column[40]. As the vivianite particles range from 10-200  $\mu$ m, this would mean that smaller minerals would end up in the tailings flow. However, several papers have shown that concentration of ultra-fine heavy particles (as fine as 10  $\mu$ m) is possible with spiral concentrators[7, 10, 22, 40, 50]. Some relevant researches are summarized below, where spiral concentrators were used to process materials having similarities to sewage sludge.

In the mining industry, the processed particles on spirals are minerals. However, for the sewage sludge, there is also a presence of organic material. These organic solids are much larger than the minerals and shaped in various ways. Spirals are capable of efficiently separating particles with similar densities, as long as there is a marked difference in shape[7]. This has been shown by Browning, who separated mica from quartz and feldspar, where flaky mica particles were swept into the fast flow at the outer rim, while quartz and feldspar settled in the inner rim[6]. Furthermore, Richards et al.[40] concentrated fine Australian silica sand, containing heavy minerals with a specific gravity of 2.85 and also an organic fraction. The reject flow contained most of the water and organics and contained ultrafine silica sand particles. 56.6% of the heavy minerals were recovered in the product. The recoveries were plotted against the cumulative mass to product (how much % of the mass goes to the product), shown in Figure 2.11. This test was performed with a so-called FM1 spiral concentrator, designed to operate down to 30 µm. For a conventional spiral, no data was available, as the flow on conventional spirals were observed to be too turbulent to effect organic separation[40].

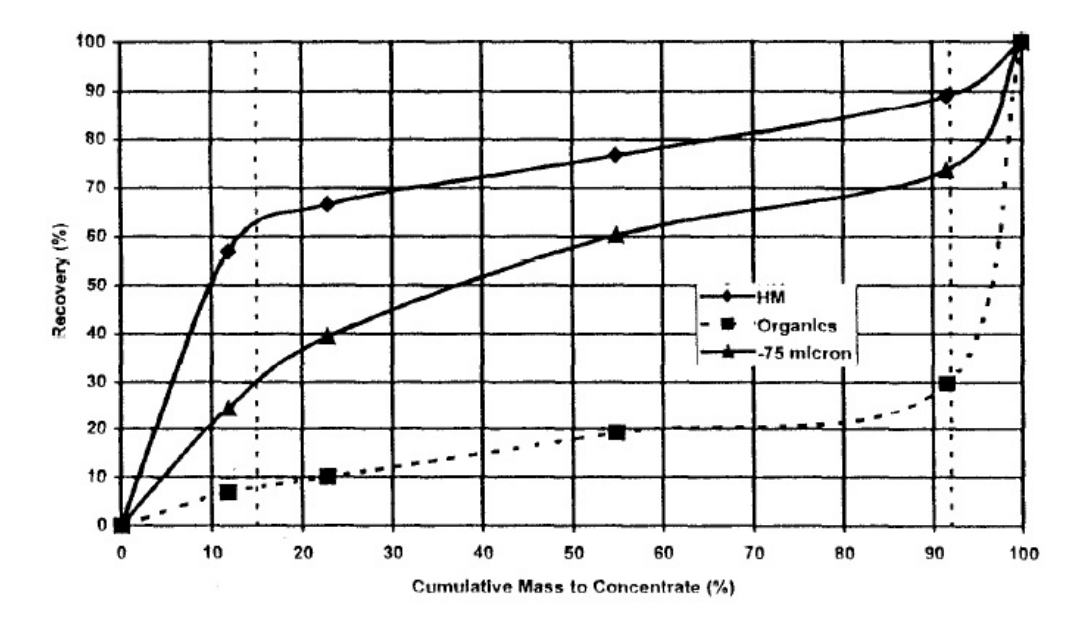


Figure 2.11: Spiral performance on Australian silica sand with Heavy Minerals (HM), organic material and ultra-fine particles (-75 μm)[40].

Ringeling et al.[41] used coal spirals to clean six batches of soil by separating organic substances, being polycyclic aromatic hydrocarbons (PAH) and other organic substances. The small axial and radial inclination make the coal spiral suitable for separation of relatively light contaminants. The soil was pre-processed with screens and with a hydrocyclone, to remove particles larger than 30 mm, and smaller than 63 µm. Furthermore, contaminants that were attached to particles, were liberated by using a high-pressure unit. For all six batches, the organic contaminants were efficiently removed, captured in the outer flow of the trough. Some of the contaminants co-existed with particles in the outer rim, slightly reducing the effective efficiency of the spiral, but the effective PAH reduction still ranged from 69-87%.

Glass et al.[14] also investigated the application of coal spirals for cleaning contaminated soil. They discovered that the recovery of organic contaminants was generally the largest in the middle flow, not in the outer flow. To find the reason behind this phenomenon, they performed experiments. To guarantee that all contaminants were free particles, polyethylene terephthalate (PET) particles were used instead of PAH, which has more or less the same density (1.4 g/cm³). Instead of soil, sand was used (2.65 g/cm³), as it has no affinity with PET, so interaction between particles was absent. These densities come close to the organic and vivianite densities in the sludge. The particle size for the experiment was maintained at 1.0 mm by screening. Slurry densities and flow rates were changed for each experiment, to research the effect of these parameters on the separation of PET and sand. It was concluded that increasing the slurry density and flow rate stimulates the contaminants to shift to the outer flow and cleans the inner flow. More sand moves to the middle flow with increasing flow rate, but with increasing density, more sand remains in the inner flow. Still, the majority of PET remained in the middle flow, which was inevitable as increasing the density and flow rate would overflow the spiral. However, the contaminants could be effectively concentrated by altering the splitter position.

For spiral concentration of fine minerals, the control of turbulence (Reynolds number) across the trough is important, so that controlled settling the flowing medium is possible[21]. The Reynolds number is given by:

$$Re = \frac{\rho * v * h}{\eta} \tag{2.22}$$

With v being the fluid velocity and h the thickness of the flow. Open channel flow is generally laminar if the Reynolds number is below 500, and turbulent if Re>1000, with a transition zone in between. Near the rim of a spiral, the flow thickness and fluid velocities are higher, resulting in a higher Reynolds

number and more turbulent flow. With increasing flow rate, the fluid velocity increases and with that the centrifugal force increases. This means that fine heavies will be forced in the more turbulent fast flowing tailing band, decreasing recovery[30]. On the other hand, low fluid flow rates will not force light particles to the outer rim as centrifugal forces will be too small. The optimal flow rate depends on the spiral and material characteristics, but for most separations, 1.0 to 1.5 L/sec for standard spirals with an outer radius of 30 cm is the optimum range[7].

Due to the relatively high viscosity of sewage sludge, the ratio of inertial stress to viscous stress *N* (Equation 2.9) is likely below 40, so within the macro-viscous regime(Figure 2.9). The high viscosity reduces the Reynolds number of the flow. Turbulent flow induces eddies, which impose a lifting force on particles and therefore increase the Bagnold force. As the Reynolds number for sewage sludge is lower than for water mixtures, the Bagnold force will be lower and lighter particles are less likely to move outwards, which will reduce the grade of the product flow. A possibility is that due to the high sludge viscosity the secondary flow on the spiral is absent. Heavy particles will still settle and move inwards, but light particles will not move outwards, so the spiral loses its function as a separator. It then functions as a thin film settler, where heavy solids are concentrated near the spiral column. This is still beneficial, as the product then has a higher solids content, but with a low grade. The magnetic separator placed after the spiral then has less fluid to process, and can increase the product grade.

# 3 Material and Methods

To research particle migrations in sewage sludge, experiments are performed. First with a centrifugal experiment, and later with a spiral concentrator. Synthetic sludge was used for the first tests. Description of sewage sludge and the synthetic sludge can be found in Section 3.1. The particle behavior in sludge is investigated with a centrifugal experiment, described in Section 3.2. Finally, the separation efficiency of the spiral is tested, as described in Section 3.3.

#### 3.1 Material selection

Digested sewage sludge characteristics constantly change by the microorganisms in the sludge, which makes it almost impossible to carry out controlled experiments in sludge studies or to reproduce test results[65]. For the first experiments, synthetic sludge is used, as this is stable and retains its quality, in contrast to sewage sludge. This makes it possible to perform multiple tests with the same synthetic sludge. Before creating synthetic sludge, the viscosity of the sewage sludge was measured. Section 3.1.1 gives the results of viscosity measurements, and Section 3.1.2 gives the composition of the synthetic sludge.

#### 3.1.1 Viscosity measurements

The viscosity of sewage sludge was measured using an Anton Paar MCR302 rheometer. It has previously been shown that sewage sludge shows shear-thinning behaviour[56], meaning that the viscosity of the sludge decreases with increasing shearing rate. Shear-thinning is most likely caused by a change of particle orientation, and organic flakes might break down into smaller flakes with higher shearing rates.

Samples were taken directly from the digester and were tested the same day. 15 ml samples were used for the rheological measurement. The rheometer has two concentric cylinders (a rotating measuring bob and stationary cup) as a rotational Couette geometry. The CC27 system was used, having a 26.656 mm bob diameter, and a 28.920 mm cup diameter. The measurement temperature was set at 20°C. The viscosity was measured with shearing rates ranging from 0.01 s<sup>-1</sup> to 1000 s<sup>-1</sup>, with a decreasing time interval from 10 s to 1 s, both varied logarithmic, as previously done by Wei et al. [56]. Before this, the material was pre-sheared for 90 seconds with a rate of 1000 min<sup>-1</sup> to reach a homogeneous sample distribution, and then paused for 30 seconds. First, the sensitivity of the rheometer settings was investigated by changing the variables and testing with the same sample. Afterwards, tests with the same variables were performed on different samples. No distinct differences were observed in both cases. Another test was performed at a temperature of 35°C, which is generally the temperature of sludge exiting the digester. This showed a slightly lower viscosity, as expected. The flow curves for both 20°C and 35°C samples are shown in Figure 3.1. On a spiral, shear rates are present over the flow velocity differences between the bottom and top of the film. This rate is generally in the order of 300-500 s<sup>-1</sup>. The synthetic sludge was given a zero shear viscosity of 0.1 Pa·s, corresponding to a shear rate of 50 s<sup>-1</sup> in Figure 3.1.

3.1. Material selection 20

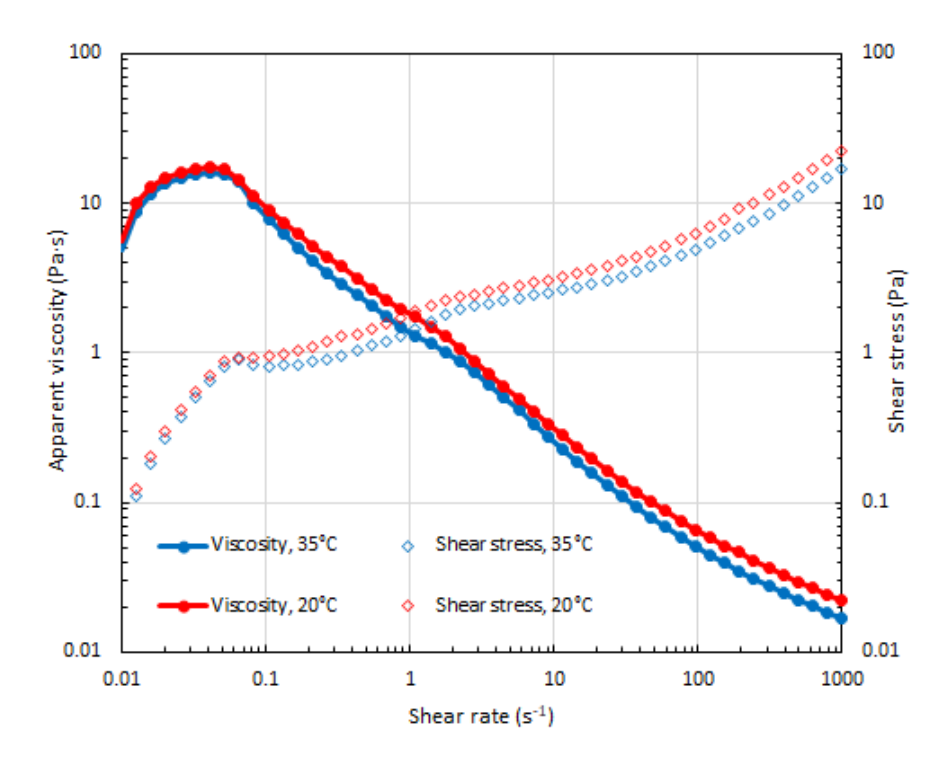


Figure 3.1: Rheograms for two sewage sludge samples with different temperatures.

#### 3.1.2 Synthetic and sewage sludge

The synthetic sludge must be representative for the real sewage sludge, and therefore needs to have comparable characteristics. Sand, having the same density as vivianite (2.65 g/cm³) represented vivianite in synthetic sludge. CEN Standard Normensand EN 196-1 was used, having a specific grain size distribution between 0.08 and 2.00 mm[36]. PET flakes represented the organic content, having a density of 1.4 g/cm³. The total solids content of the synthetic was 4% wt, of which 30% sand and 70% PET. The right viscosity was created by mixing water and glycerol. The viscosity of a Newtonian slurry ( $\eta_m$ ) with a known solid volume fraction (C) and liquid viscosity ( $\eta_l$ ) can be determined with the formula found by D.G. Thomas[49]:

$$\eta_m = \eta_l (1 + 2.5C + 10.05C^2 + 0.00273e^{16.6C}) \tag{3.1}$$

As the solid volume concentration is known for the synthetic sludge, the water/glycerol mixture viscosity can be calculated to obtain the desired sludge viscosity. To create a sludge with a zero shear viscosity of 0.1 Pa·s with a solids weight concentration of 4%, the volumetric water/glycerol ratio is approximately 1:4, determined with an online calculator[54].

The synthetic sludge was not used in the centrifuge, as the PET flakes are too large to properly migrate through the thin film. Two different synthetic sludges were used for spiral testing, differing in solid particle sizes. For each experiment with sewage sludge, the sludge was sampled from the Nieuwveer STP and experimented with on the same day, to avoid changes in sludge characteristics that occur over time. The sewage sludge characteristics are previously described in Section 2.1.5.

# 3.2 Centrifugal experiment

The experimental setup is based on centrifugal separation and will be referred to as a centrifuge in the following. The centrifuge consists of a cylinder, attached to a drill with disks that generates the rotational movement. The cylinder is open at both ends. Sludge is fed into the cylinder at a constant rate with a pump that is installed above the cylinder. Because of the rotation of the centrifuge, a thin fluid film will form on the inner surface. At the bottom of the cylinder, a splitter is installed to split the film into two flows. The splitter position is adjustable. Furthermore, the fluid flow rate and the rotation speed can be altered.

#### 3.2.1 Definitions

In this study, the flow that is collected with the splitter is called the tailings flow, while the flow on the cylinder surface, unaffected by the splitter, is called the product flow. The initial mix that is poured in the system is called the feed. The grade is the purity in terms of dry weight, and the recovery is the amount of a material recovered in the product compared to the initial quantity in the feed. The total solids (TS) content is the dry solid weight divided by the weight of the wet sample, so the solids concentration of a sample. The volatile solids content (VS) is the weight reduction after igniting a dry sample, divided by the initial dry weight. Volatile solids are all solids that are removed after heating in an oven, so generally organic material, but also crystals waters from minerals. Finally, the non-volatile solids content (non-VS) is the weight left after igniting a sample, divided by the initial dry weight. These are minerals present in sludge, such as vivianite and quartz. The method used to determine the TS and VS content is given in Section 3.2.4.

# 3.2.2 Theory

In the magnetic separator, vivianite particles are migrated over a small distance (1 mm) by a magnetic force and are recovered when they reach the magnetic plates. In the centrifuge the migration distance is similar, but this migration is created by centrifugal forces acting on the vivianite minerals. The goal of the centrifuge is to let vivianite migrate towards the cylinder surface, while organic material retains its position. The splitter will then cut the vivianite rich flow near the surface, and separate it from the organic-rich residue. Along the cylinder length, the film thickness is constant. At the cylinder surface, the vertical fluid velocity will be zero and will be maximum at the air interface, having a parabolic velocity profile as the flow is laminar, shown in Figure 3.2. Knowing this, the Navier-Stokes equation can be solved for v(x), the flow velocity v at radial distance v:

$$v(x) = \frac{\rho_f a}{2\eta} x (2d_{film} - x) \tag{3.2}$$

Where a is the acceleration parallel to the cylinder surface, and  $d_{film}$  the film thickness. The average velocity  $\overline{v}$  can then be calculated by integrating v(x), giving the following formula:

$$\overline{v} = \frac{\rho_f a}{3n} d_{film}^2 \tag{3.3}$$

The terminal velocity of spherical particles in a centrifuge is given by the following equation[18]:

$$v_t = \frac{D_p^2(\rho_p - \rho_f)\omega^2 r}{18n} \tag{3.4}$$

Where  $\omega$  is the angular velocity. With a given residence time, the radial displacement (dx) of a particle can be determined. Assumed is that the terminal velocity does not change with increasing radius, as the displacement is limited (only a few mm). A particle travels distance dx in radial direction, and the length of the cylinder (H) in vertical direction. Figure 3.2 shows the cross-section of a centrifuge,

including dx and H. All particles that are able to migrate towards the cut position will be recovered. In the figure, this is given as  $x_0$ , all particles within this distance will be recovered. To determine the distance  $x_0$ , the following equation can be used:

$$H = \frac{\rho_f \alpha}{2\eta} \int_{x=cut}^{x_0} x(2d_{film} - x) \frac{1}{v_t} dx$$
 (3.5)

Where  $dx/v_t$  is the residence time. Assumed is that the particles are initially homogeneously distributed. The recovered particles will then be in the film between x=0 and  $x=x_0$ , thus the total recovery can be given with the following formula:

$$Recovery = \frac{\int_{x=0}^{x_0} v(x)dx}{\int_{x=0}^{d_{film}} v(x)dx}$$
(3.6)

As the displacement dx depends on the particle size, the recovery changes with particle size. For a prediction of the total recovery, the particle size distribution would be needed. Note that  $\eta$  in all equations above is not a constant, but a relation dependent on temperature and shearing rate as shown in Figure 3.1.

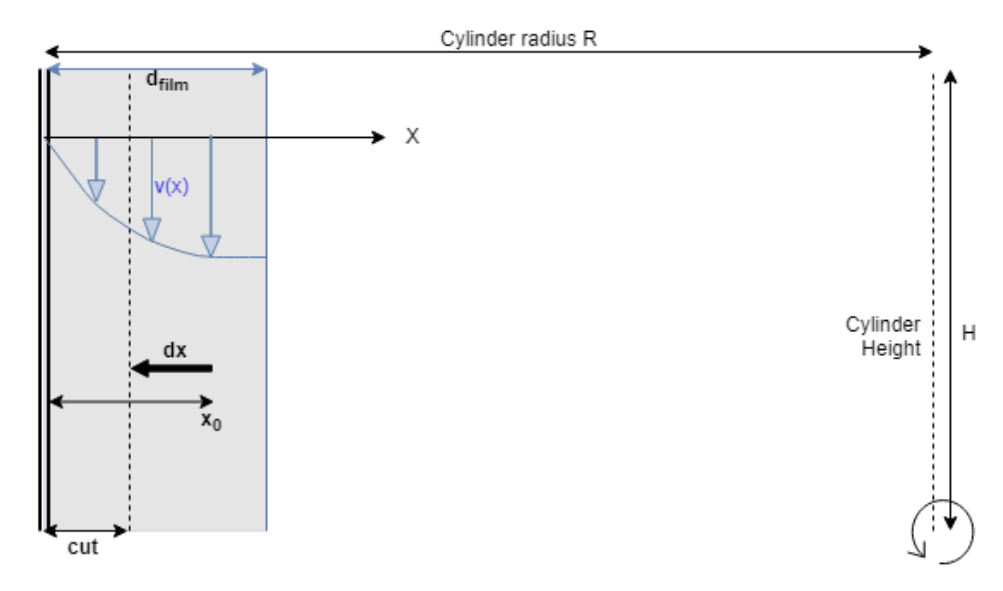


Figure 3.2: Schematic cross-section of the centrifuge.

#### 3.2.3 Dimensions

A sketch of the centrifuge setup is shown in Figure 3.3, and an image of the setup is shown in Figure 3.4. The cylinder has a length of 39.6 cm, with a diameter of 24 cm. The cylinder is attached to the drill with two disks. The drill has the following operational settings: 560, 800 or 1350 rpm and rotates clockwise seen from above, exerting a force of 42, 86 and 245G on the cylinder respectively. Below the cylinder, a collecting tank is installed with the splitter attached to it, this tank can be moved to alter the splitter position. The splitter cuts and collects the tailings flow in a pipe, while the product is collected in a funnel to enable sampling, and then transported to the tank with tailings material. The material is then pumped back into the cylinder to create a closed-loop circulating system. The flow rate of the feed can be changed manually with the frequency controller connected to the pump.

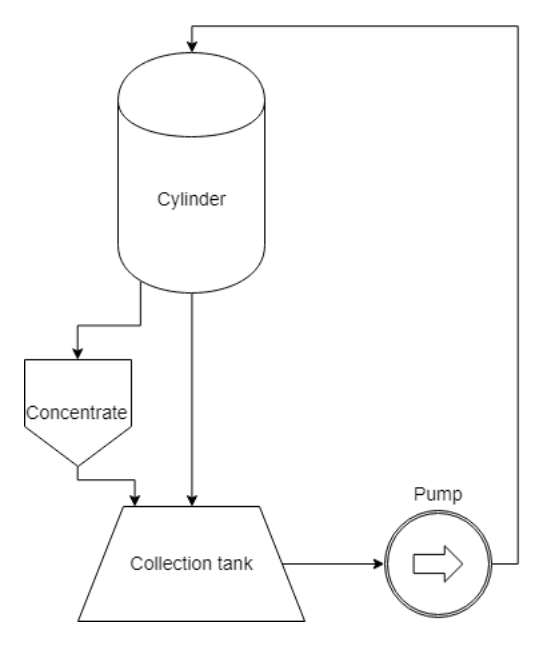


Figure 3.3: Diagram of the centrifuge setup.

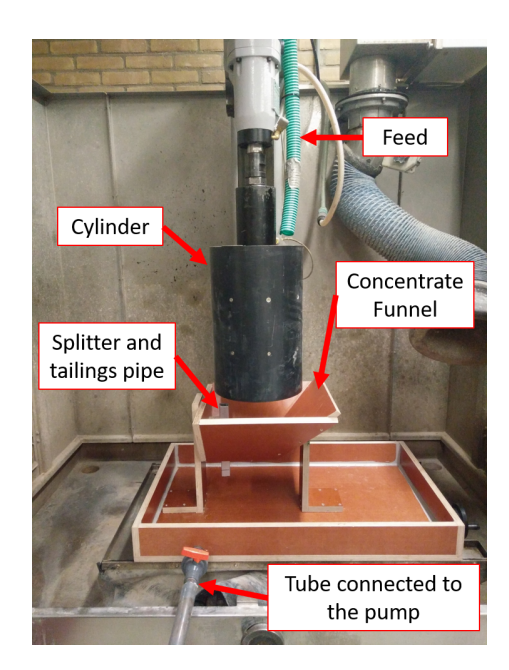


Figure 3.4: The centrifuge setup at the start of an experiment.

### 3.2.4 Sample analysis

Feed samples were taken in triplicate from the pump outlet before centrifuging, and the feed rate was determined. The drill was then started and samples from the tailings and product flows were taken in triplicate too. Next to that, the tailings rate was determined. All of this was repeated for different splitter positions.

For sewage sludge, determination of vivianite recovery is difficult. The exact concentration is hard to determine with X-ray diffraction spectroscopy (XRD), as vivianite has impurities and the minerals can be amorphous. Furthermore, X-ray fluorescence (XRF) also has its limitations, as the phosphorus can be partially be bound to other minerals than iron, and not all the iron is necessarily bound to phosphorus, so with an elemental composition of the sludge, the vivianite content cannot be estimated. Possibly, a combination of XRD, XRF, and Mössbauer spectroscopy could give a good estimation of vivianite content. Another option is to magnetically separate the vivianite several times, to retrieve all vivianite from the sludge. Both options are investigated in another study.

In this study, only total solids and the volatile solids of the samples will be measured, according to standard methods[2]. The samples were dried by placing them under an air blower. Normally, one would place them on a water bath at 100°C, but as vivianite already loses 25% of its weight around 100°C due to loss of crystal water[66], these samples were dried at room temperature. The dry samples were heated in an oven to 550°C, to determine the volatile solids content. The remaining dry solids consist of different minerals such as quartz and vivianite, so the exact vivianite concentration cannot be determined with this analysis. Additionally, samples were taken for analysis with inductively coupled plasma optical emission spectrometry (ICP-OES). This method measures the elemental composition of a sample. For each element, the concentration is given in % of dry solids (ds). The exact vivianite concentration cannot be determined with ICP-OES, as not all P is necessarily bound to Fe or vice versa.

### 3.3 Spiral concentration experiments

An industrial size spiral concentrator was used for the spiral experiments. The spiral type and dimensions are given below, together with relevant definitions and the testing procedure and analysis methods.

#### 3.3.1 Definitions

The spiral has three outlets at the bottom. The inner outlet, most close to the column, is called the product flow. The flow in the middle is called the middlings, and the outer flow is called the tailings. Feed, grade, recovery, TS, VS, and non-VS are previously defined in Section 3.2.1. Furthermore, yield is defined as the % of total material, either sludge or solids, ending up in a single outlet.

#### 3.3.2 Dimensions

The used spiral is a double stage Multotec MX7 coal spiral, consisting of 7 turns, with a pitch u of 43 cm, an inner radius  $r_i$  of 77 mm and outer radius  $r_o$  of 50 cm. The spiral is developed for difficult to wash coals, for a size range of 2.0 to 0.1 mm[35]. This spiral has been chosen for its relatively shallow inclination and a large number of turns, increasing the residence time. The trough contains a deeper reject channel directly next to the column, which concentrates large and high density particles. This channel is called a gutter in the following. The trough profile is shown in Figure 3.5. A repulper is present halfway down the spiral, which remixes the outer flow (middlings and tailings), while the product flow remains the same. How much of the outer flow is remixed, can be altered with an auxiliary splitter. As the flow is remixed halfway, this spiral is called a double-stage spiral. The first stage consists of four complete turns, the second stage of three when it reaches the splitter box. The splitter box divides the flow into product, middlings, and tailings.

The spiral circuit is visualized in Figure 3.6 and an image of the setup can be found in the Appendix (Figure B.2). Material from the product, middlings, and tailings flow is collected in a tank below the splitter box, where it is mixed and pumped to the top of the spiral with a Jabsco impeller pump. It is pumped into a head tank which has a feed and overflow port. The overflow goes back to the collection tank, while the rest of the material is fed onto the spiral with a controlled flow rate by using a frequency controller connected to the pump. A bypass is installed at the tank level to permit sludge circulation when emptying the tank.

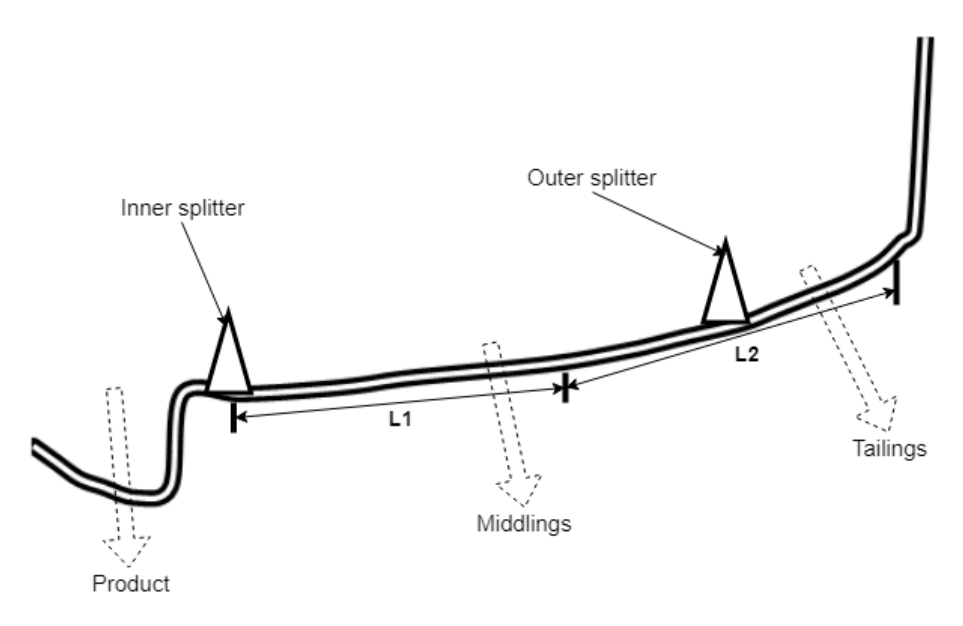


Figure 3.5: Spiral trough and splitter ranges L1 & L2.

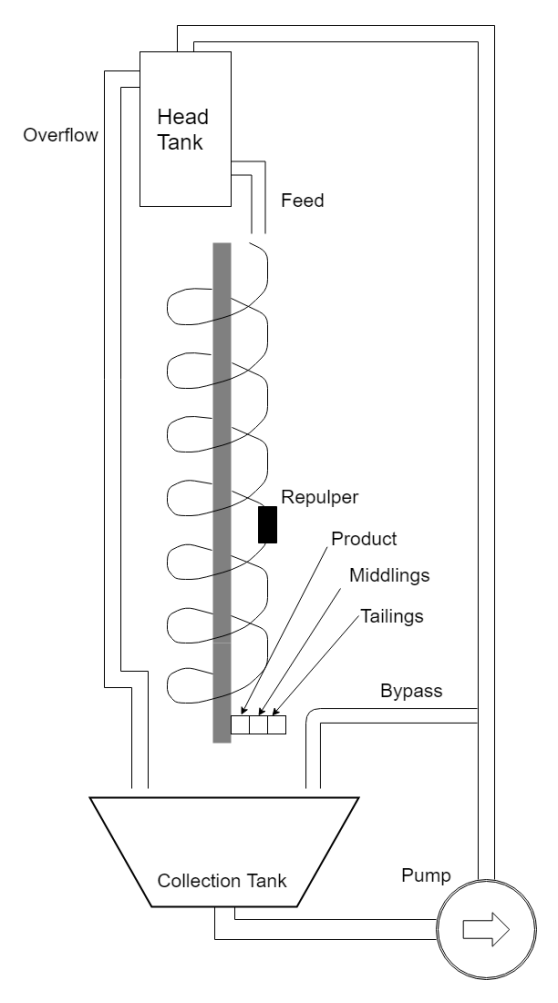


Figure 3.6: Diagram of the spiral test setup.

### 3.3.3 Spiral testing

The feed rate and splitter positions were the only variables during experiments. The position of the auxiliary splitter of the repulper was set at 31 cm from the outside rim for all tests. The ranges of the inner splitter L1 (13 cm) and outer splitter L2 (16 cm) of the splitter box are shown in Figure 3.5. The splitters were moved over these ranges to investigate their influence on the grade and recovery of the product, middlings, and tailings. Three splitter configurations were used for both the tests with synthetic and sewage sludge, these are shown in Figure B.3. The default position is where both splitters are set the nearest towards the spiral column, with openings of 10, 13 and 15 cm for the product, middlings and tailings flow respectively. Before each experiment, the material was circulated for a few minutes to create a stable circulating system and feed samples were taken from the top of the spiral. Then for each splitter configuration, the flow rate in g/s of each outlet is measured. First, all material is collected in a large bucket and timed, to determine the total feed rate in g/s. Then three containers are simultaneously slid under the outlets and weighted afterwards, to determine what fraction of the feed rate ends up in each outlet. Afterwards, samples from each outlet are taken in duplicate. The feed rate is then altered with the frequency controller of the pump and the procedure is repeated.

The synthetic sludge samples were rinsed from glycerol, dried and the sand was separated from the PET flakes by sieving. The sand is sieved for multiple mesh sizes which are weighted separately, to create a particle size distribution. For tests with sewage sludge, experiments are started by taking feed samples. Next to that, a product, middlings and tailings sample was taken for each feed rate with the default splitter configuration for ICP-OES analysis. The TS and VS of the samples are analyzed in the same manner as described in Section 3.2.4.

## 4 Results

The following chapter shows the results obtained from the centrifugal experiment and spiral concentration experiments. Spiral tests were performed with synthetic sludges and digested sewage sludge. Sewage sludge was also diluted to reduce the sludge viscosity, the effect of this on the separation process was investigated.

## 4.1 Centrifugal experiment

Centrifugal experiments were performed to investigate the behaviour of vivianite particles moving through a thin sludge film. The drill was set at 1350 rpm, resulting in a G-force of 245 on the cylinder. Before testing, the splitter distance was set at a distance of 1.0 mm from the cylinder surface. While centrifuging, the feed rate was increased until a tailings flow could be observed. This rate was 1.17 L/s. The tailings flow rate and samples from the feed, product and tailings were taken in triplicate. This was repeated for a splitter distance of 0.75 mm and 0.25 mm with the same feed rate. This resulted in a sludge yield to product of 98% (1.0 mm), 85% (0.75 mm) and 80% (0.25 mm). The TS and VS content of the samples were measured and are shown in Table A.1 in the Appendix. Figure 4.1 shows the average VS and non-VS content of the feed, product and tailings samples taken for each splitter distance. The y-axis gives the total solids concentration.

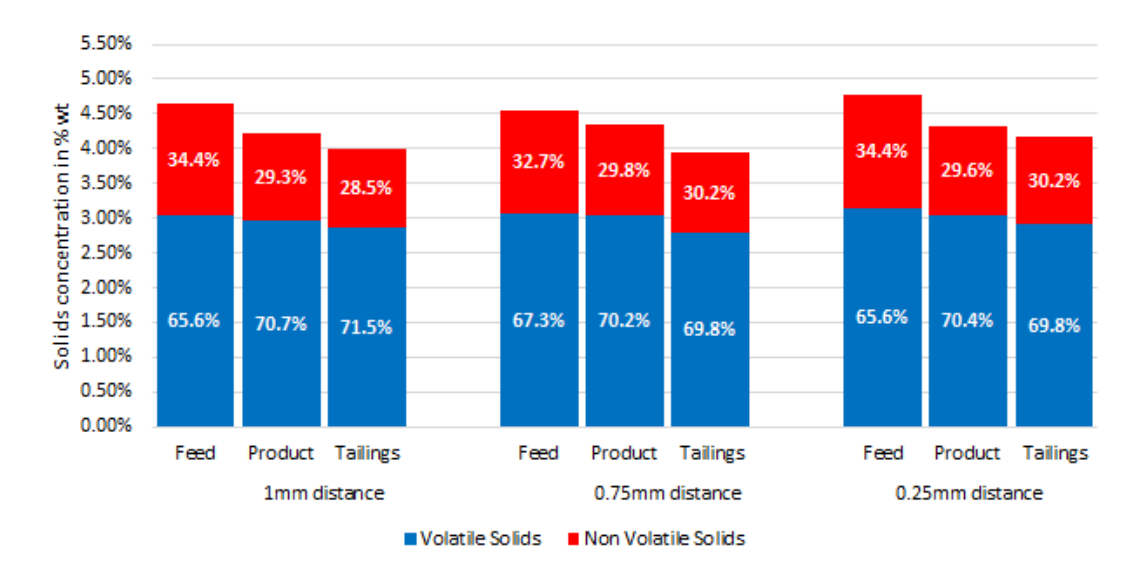


Figure 4.1: Volatile and non-volatile solids content of the feed, product and tailings samples per centrifuge splitter distance. Data labels indicating the fraction of solids.

Figure 4.1 shows that the TS of the product is larger than for the tailings for each splitter distance. The VS content of the product and tailings samples do not show significant differences. Desirably, one would see a high VS content in the tailings sample, and a low content in product samples. The splitter distance seems to have no effect on TS or VS content, neither for the product nor tailings samples as for each distance, the charts look similar.

A remarkable observation is that the feed samples have a higher TS and non-VS content for all splitter positions. Feed samples were taken without centrifuging, while tailings and product samples were taken while centrifuging. Somehow, the solids content decreases when the cylinder is rotated. The same was observed in an earlier experiment, where the splitter was not used, but samples were

taken without rotating the cylinder and while rotating it. Here the samples taken without centrifuging contained more solids and a lower VS content than the samples taken while centrifuging, as shown in Table 4.1. These samples were also analyzed with ICP-OES analysis. The sample taken without centrifuging contained more Fe and P than the other samples. This table shows average values, all values can be found in Table A.2. Even without splitting the film, the sludge exiting the centrifuge contains 13% less solids than the feed, and 33% and 23% less Fe and P respectively.

Table 4.1: Average VS, TS, Fe and P content of samples taken without and while centrifuging.

	TS in % wt	VS in % of TS	Fe (mg/g ds)	P (mg/g ds)
Without centrifuging	4.16	66.76	58.68	30.14
While centrifuging	3.61	71.02	45.51	26.69

A possible cause for the differences in samples taken while and without centrifuging, could be that during centrifuging vivianite minerals migrated towards the cylinder surface and stuck to the surface without moving downwards. The centrifugal force and friction with the surface would be too large to let the minerals move downwards with gravity and exit the cylinder. Fewer solids would then escape the system, the VS content would be higher and there would be a reduction in Fe and P concentration. Table 4.1 shows a larger reduction in Fe than in P. This could be explained by the mass ratio of Fe and P in vivianite. In vivianite, the Fe mass is 2.7 times higher than the mass of P. Besides vivianite, other minerals such as quartz, pyrite and siderite might have gotten stuck on the cylinder surface too, where pyrite and siderite would reduce the Fe content even more.

Using the formulas in Section 3.2.2 and the known parameters (cylinder dimensions, rotational velocity, feed rate, densities & viscosity curve), the theoretical vivianite recovery for different particle sizes can be computed, as shown in Figure 4.2. Here a recovered mineral is a mineral that has reached the cylinder surface within the residence time in the cylinder. Note that the recovery here does not represent the total recovered vivianite, but how much is recovered per particle size. Theoretically, all vivianite particles larger than 100 µm will have migrated the total film thickness, meaning a recovery of 100% for this size. According to this graph, and the knowledge that vivianite particles are between 10-200 µm[62], a part of the vivianite minerals should have reached the cylinder surface, what the experimental data also suggests. The exact recovery cannot be determined, as particle size distributions of vivianite in sludge are unknown. The terminal velocity (Equation 3.4) assumes unhindered movement for spherical particles. However, vivianite minerals are not spherical and are likely hindered by other particles such as organic fibers. Therefore a shape factor and tortuosity factor of 0.5, so a total factor of 0.25, were used to plot Figure 4.2.

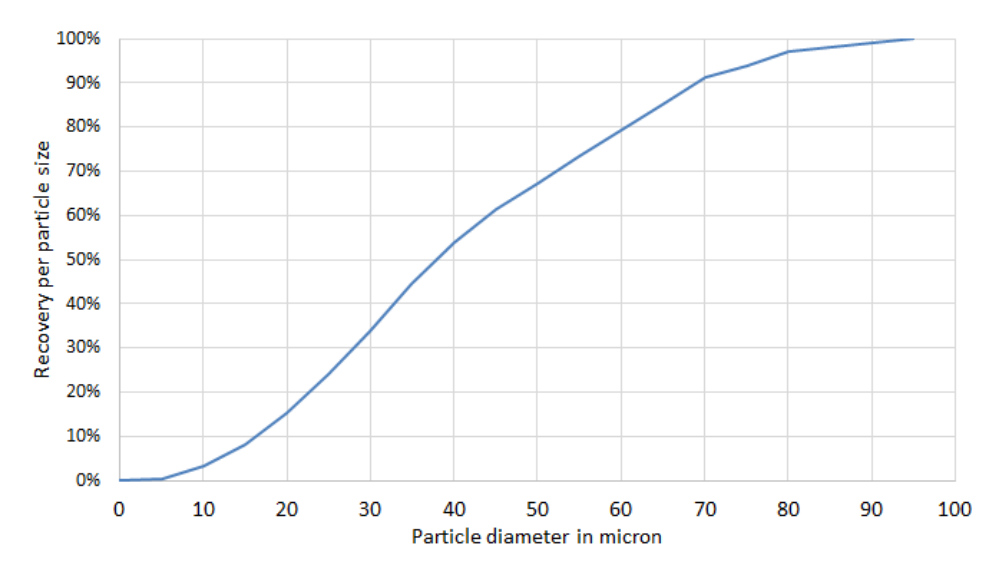


Figure 4.2: Theoretical vivianite recoveries for different particle sizes.

### 4.2 Spiral concentration with synthetic sludge

To test the spiral with a stable viscous mixture, synthetic sludge was created with sand and PET particles, having similar densities as vivianite and organics in sewage sludge. Due to an error, the synthetic sludge was mixed with a zero shear viscosity of 0.025 Pa·s for all experiments on the spiral, instead of 0.1 Pa·s that was determined in Section 3.1.2. Viscosity measurements showed that for shearing rates higher than 1 s<sup>-1</sup>, the viscosity remained constant at 0.01 Pa·s, shown in Figure A.1. Tests were performed with two different mixtures; one with sand particles of 0.08-2.0 mm and PET flakes of 2.3-7.0 mm, and the second mixture with sand particles of 10-200 µm and PET particles around 1 mm. Both mixtures had the same viscosity. Results of both tests are described below.

### 4.2.1 0.08-2.0 mm sand particles & 2.3-7.0 mm PET flakes

The first experiment with synthetic sludge was performed with a sludge consisting of PET particles of 2.3-7.0 mm and sand particles with a known size distribution between 0.08 and 2.0 mm. For this experiment, the sand particle size distributions of the product flow were determined for different feed rates. These are plotted in Figure 4.3, together with the original particle size distribution of feed.

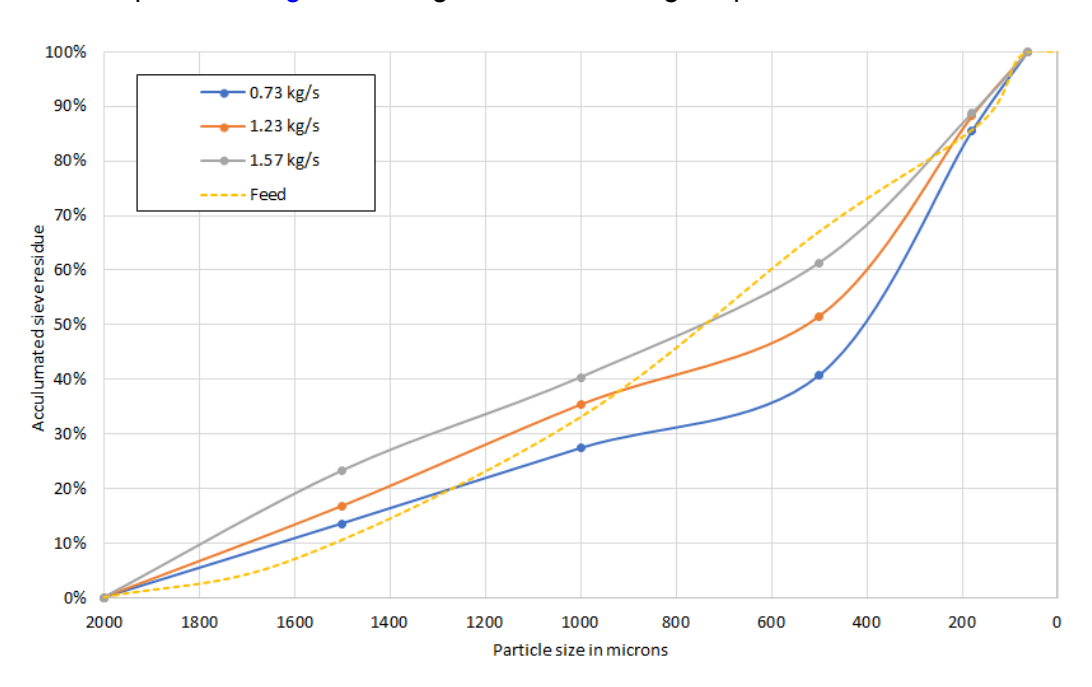


Figure 4.3: Particle size distributions of sand in the product for three different feed rates.

This figure shows that with an increasing feed rate, the fraction of large particles in the product increases. This is caused by a decrease in smaller particles content for higher feed rates. As expected, higher feed rates caused higher fluid velocities and higher centrifugal forces, forcing smaller particles to migrate outwards towards the tailings flow. The particle sizes of this mixture do not represent particles in sewage sludge well, but by using this large variety in sizes, the effect of feed rate on different particle sizes could be determined.

#### 4.2.2 10-200 µm sand particles & 1 mm PET flakes

The second experiment was performed with sludge that contained sand particles of 10-200  $\mu$ m and PET flakes of 1 mm, which represent the particles in sewage sludge better. This sludge was tested with the same feed rates as the previous experiment, and samples were taken for different feed rates and splitter configurations. Results for the default splitter configuration (position A in Figure B.3) are shown in the table below.

	Fluid yield in %	Solids yield in %	Sand recovery in %	Grade in %
		Feed rate	= 0.73 kg/s	
Product	20.9	24.1	80.1	56.1
Middlings	41.0	24.6	18.7	12.8
Tailings	38.1	51.3	1.1	0.4
_		Feed rate	= 1.23 kg/s	
Product	22.0	33.4	89.3	75.5
Middlings	25.5	16.1	9.6	16.7
Tailings	52.5	50.5	1.1	0.6
		Feed rate	= 1.57 kg/s	
Product	18.8	34.8	90.4	77.7
Middlings	20.3	8.6	4.5	15.7
Tailings	60.9	56.5	5.1	2.7

Table 4.2: Results from the spiral experiment with synthetic sludge, 10-200 μm sand particles & 1 mm PET flakes.

The table shows that with increasing feed rate, the fluid fraction captured in the product outlet remains similar, the fraction in the middlings decreases, while a large increase is seen in the tailings outlet. The solids yields, on the other hand, show different behaviour. With increasing feed rate, the fraction of solids in the product flow increases, it decreases in the middlings and remains similar in the tailings. Looking at the sand recovery, the same behaviour is observed. Only the tailings recovers more sand for a feed rate of 1.57 kg/s, this could be caused by the smaller sand particles that are forced outwards due to an increase in centrifugal force, which was also observed in the previous section. The grade of the product also increases with an increasing feed rate. With a feed rate of 0.73 kg/s, only 56.1% wt of the solids in the product were sand particles, but this increases to a grade of 77.7% for a feed rate of 1.57 kg/s. As plastic flakes are more prone to move to the outer flow with increasing feed rate, the grade of the product increases.

In the mining industry, the fluid yield is generally not of importance as water is easily removed. However, with sewage sludge liquid removal is a costly operation. Therefore the spiral would ideally recover the least amount of liquid with as much solids possible in the product flow. To define the best operational parameters, some plots can be made that visualize the spiral performance, which are shown in the following section.

### 4.2.3 Spiral performance

To visualize the performance of a spiral, three different plots can be used. The yield-recovery curve, shown in Figure 4.4, plots the recovery on the y-axis against the total sludge recovered on the x-axis. The lower limit of this plot is a linear line, representing zero efficiency where the grade of the product is always equal to the feed grade, and therefore represents no efficient separation. The recoveries of sand and PET are plotted for three different feed rates. This plot clearly shows the effect of changing splitter positions (fluid recovery) on the mineral recovery. For a sludge yield of 25%, more than 80% of sand is recovered, while the PET recovery is low. A feed rate of 1.57 kg/s shows the best plot, having a recovery of 90% for a yield of only 19%. The limitation of this plot is that the product grade is not presented.

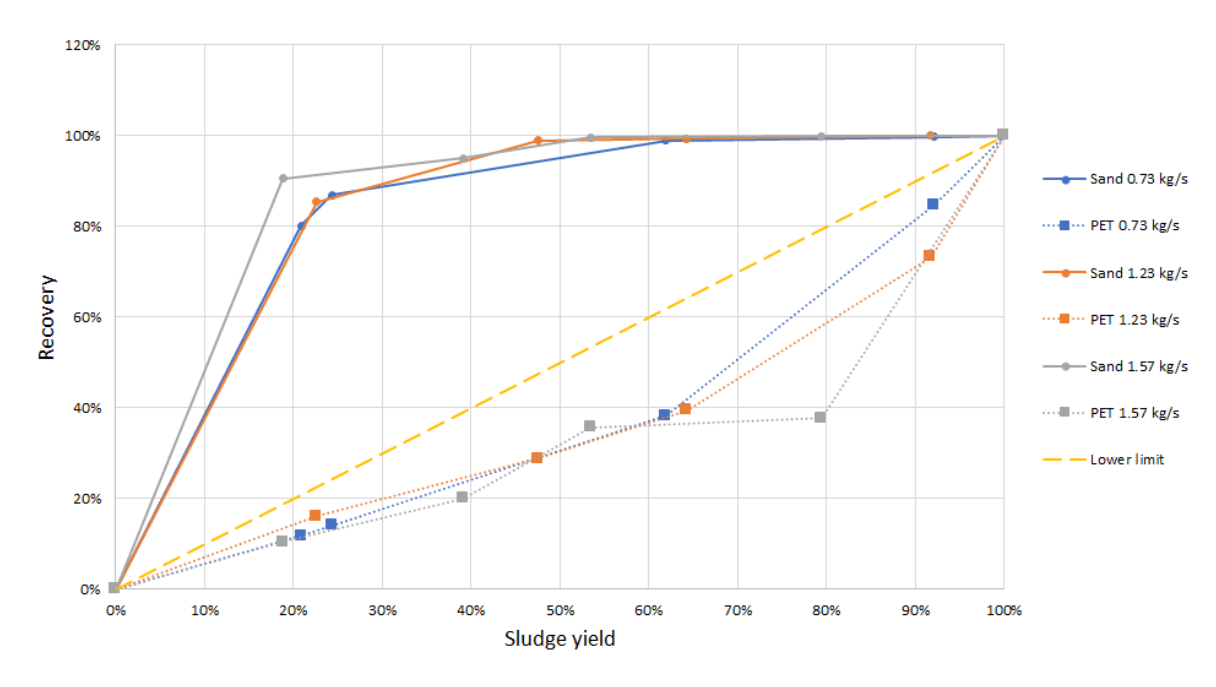


Figure 4.4: Sand and PET recovery curves for three different feed rates.

Another useful plot, which does take the product grade into account, is the yield-enrichment plot, shown in Figure 4.5. Here the total sludge yield is shown on the x-axis, and the product enrichment, being the ratio between the product grade and the feed grade, on the y-axis. This graph lacks the total mineral recovery and therefore needs to be used in combination with the yield-recovery plot. For all feed rates, the enrichment is highest for a low sludge yield, which is expected as more PET is recovered when the sludge yield increases, shown in the recovery plot.

Figure 4.6 shows the efficiency of a spiral, plotted against the *solids yield* on the x-axis. The efficiency of a spiral can be determined with the following equation:

$$E = \frac{R - W}{1 - f} \tag{4.1}$$

With R being the mineral recovery, W the total solids recovery and f the feed grade. For a perfect separation, the efficiency is 100% for a solids recovery that is equal to the feed grade. For the synthetic sludge, the feed grade f of the mixture is around 30%, the peak of the perfect separation plot. The graph shows that a lower feed rate gets closest to a perfect efficiency plot.

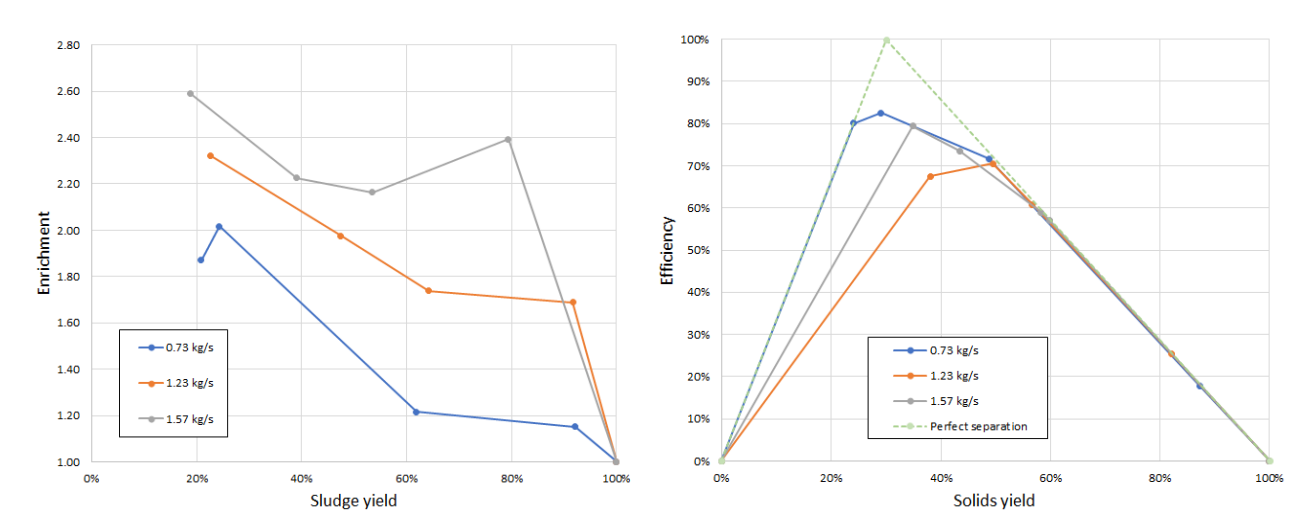


Figure 4.5: Sand enrichment for three different feed rates.

Figure 4.6: Spiral efficiency for three different feed rates.

## 4.3 Spiral concentration with sewage sludge

The next experiments were performed with digested sewage sludge, which was sampled in June 2019 from the Nieuwveer STP and tested the same day. To investigate the influence of the spiral operation parameters, the feed rate and splitter positions were altered during testing. The following sections show the results obtained from the solids and ICP-OES analysis.

### 4.3.1 Solids and elemental analysis

Feed samples were taken in triplicate, which showed an average TS content of 4.86% and a VS content of 68%. The Fe and P concentrations of the feed were 45.1 and 31.1 mg/g dry sludge respectively.

Table 4.3 shows the results from the solids and elemental analysis for the default splitter configuration. The used feed rates were approximately 0.9 kg/s, 1.2 kg/s and 1.4 kg/s. With increasing feed rate, the fraction of the flow to the product outlet decreases, remains similar in the middlings and increases in the tailings outlet. It was observed visually that with an increasing feed rate, more of the trough surface was covered with sludge towards the outer rim. In g/s, the product flow rate decreases with increasing feed rate, while the middlings and tailings flow rates increase.

For each feed rate, the TS content is highest in the product flow, meaning that solids have concentrated towards the inner flow. The differences, however, are small. Also the VS content of product samples was still high, but generally lower than for the middlings and tailings flow. The phosphorus concentration in the product flow is similar to the middlings and tailings for each feed rate, so the grade for each outlet is similar. This experiment did not show an efficient separation whatsoever, and therefore it is unnecessary to plot performance graphs.

The solids contents of the different samples are shown in Figure 4.7, with the solids concentration on the y-axis and the data labels indicating the fraction of volatile and non-volatile solids in percentage. For the first two feed rates, the TS content decreases from the product to the tailings flow, but at a feed rate of 1.4 kg/s, the lowest TS content is in the middlings flow. The graph furthermore shows that the VS content is relatively similar for all samples, suggesting that no separation has taken place between minerals and organic particles.

Table 4.3: Results from solids and elemental analysis of the spiral experiment with sewage sludge.

	Sludge yield in %	Solids yield in %	TS in %	VS in % of TS	Fe in mg/g ds	P in mg/g ds	P recovery in %
			Sludge fe	ed rate =	0.9 kg/s		
Product	63	64	4.87	67.13	46.67	31.49	64
Middlings	36	35	4.57	67.75	44.92	32.20	36
Tailings	1	1	4.58	70.08	45.67	32.60	1
-			Sludge fe	ed rate =	1.2 kg/s		
Product	46	47	4.98	66.97	47.89	31.93	48
Middlings	36	37	4.73	71.39	45.01	31.90	35
Tailings	18	16	4.51	68.60	44.96	32.36	17
			Sludge fe	ed rate =	1.4 kg/s		
Product	42	43	5.45	69.06	47.33	31.56	44
Middlings	37	35	4.78	68.93	43.65	30.75	34
Tailings	20	22	5.38	73.10	45.96	33.27	22

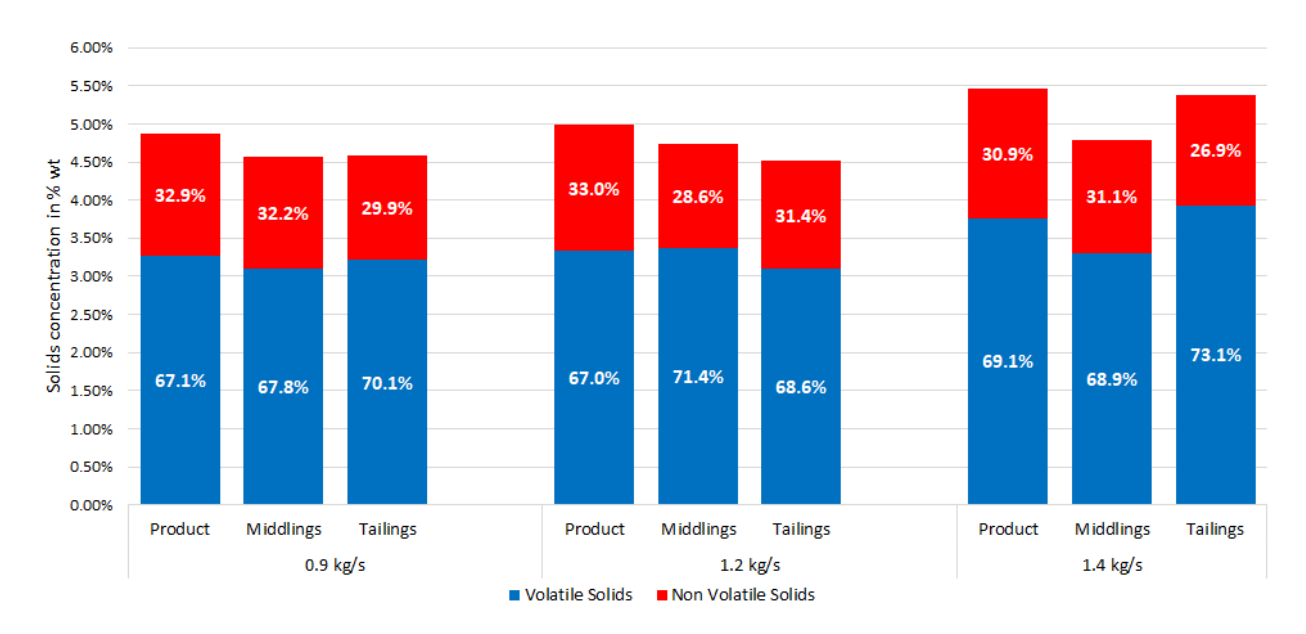


Figure 4.7: Volatile solids and non-volatile solids contents of the product, middlings and tailings samples for three different spiral feed rates. Data labels indicating the fraction of solids.

### 4.3.2 Influence of repulper

To investigate the influence of the repulper, which remixes the tailings and middlings in the fourth turn of the spiral, samples were taken from the third turn of the spiral, before the flow is remixed. The results are shown in Figure 4.8 for the highest feed rate. A clear difference can be seen between the product, middlings and tailings samples. The TS content of the product is almost 10%, with a VS content of 65.67%, while the tailings sample has a TS of 2.7% and a VS of 67.83%. The flow rates per flow could not be measured halfway down the spiral, so the fluid yield and recoveries could not be determined.

In the third turn of the spiral solids have concentrated near the column, while at the end of the spiral, the solid concentration is almost equal for all outlets. This is likely caused by the repulper located in the fourth turn of the spiral. Figure 4.9 shows how the sludge flow is redirected by the repulper. Part of the flow is sent towards the column, where it ends up in the gutter and remains here till it reaches the bottom of the spiral. The rest of the flow is remixed and exits the repulper near the rim of the trough. The remixed material flows down the spiral again, and part of it quickly flows towards the column. It was observed that the flow covers 90% of the trough radially before the repulper, while this is only 80% after the repulper. In other words, the flow becomes less wide after the repulper, which is shown in Figure B.4.

The product flow that has a 10% solids concentration before the repulper dilutes when it reaches the repulper, because part of the middlings flow is directed towards the column and therefore the solids concentration decreases. This also explains the fact that the flow becomes less wide after the repulper. The amount of sludge in the gutter increases, so the amount on the rest of the trough decreases. When the flow reaches the repulper, the middlings and tailings are remixed, and part of this mixture with a low solids concentration quickly moves towards the column and ends up in the product flow, which also decreases the product solids concentration. This shows that the repulper negatively influenced the separation process, and therefore it was removed for forthcoming experiments. During the experiments with synthetic sludge, the repulper had a smaller impact, as almost all sand had already separated from the PET before the sludge reached it. The repulper might have lowered the grade of the product slightly, as some PET flakes might have been forced to flow in the inner gutter from where they could not escape.

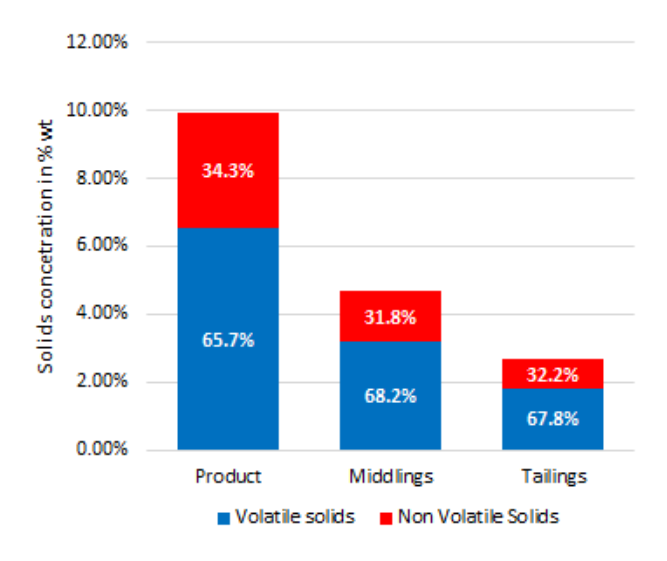


Figure 4.8: Volatile and non-volatile solids contents of the product, middlings and tailings samples taken from the third turn of the spiral. Feed rate of 1.4 kg/s.



Figure 4.9: Image of the repulper, red arrows indication how the flow is redirected.

## 4.4 Spiral concentration with diluted sewage sludge

As the results from Section 4.3 showed no effective separation, an additional experiment with diluted sludge was performed. By diluting the sludge with water the viscosity decreases, which increases Reynolds numbers and could improve the separation process. The results from tests with synthetic sludge furthermore showed that with a viscosity of 0.025 Pa·s an effective separation does take place. Because the repulper harmed the separation process of sewage sludge, it was removed from the spiral.

Firstly, samples were taken from the feed, product, middlings and tailings for undiluted sludge, to investigate the effect of removing the repulper. Then 5 L of tap water was added to the 50L of sludge, and samples were taken for different feed rates and splitter positions. This was repeated twice, so the final samples were taken from a mixture of 15 L water and 50 L of sludge. Additionally, samples from each water-sludge mixture were analyzed with a rheometer to measure the effect of diluting sludge on its viscosity. The results from the rheological tests are shown in Figure 4.10. It shows that diluting the sludge reduces the viscosity of the mixture quite linearly. Adding 5 L of water to the mixture reduces the viscosity 20-30%, with the larger reduction for lower shearing rates. The undiluted sludge shows

a slightly different curve. This plot was measured with a sludge that was sampled on a different day at the STP, which could explain this difference. The following sections show the results from spiral experiments with the diluted sludges.

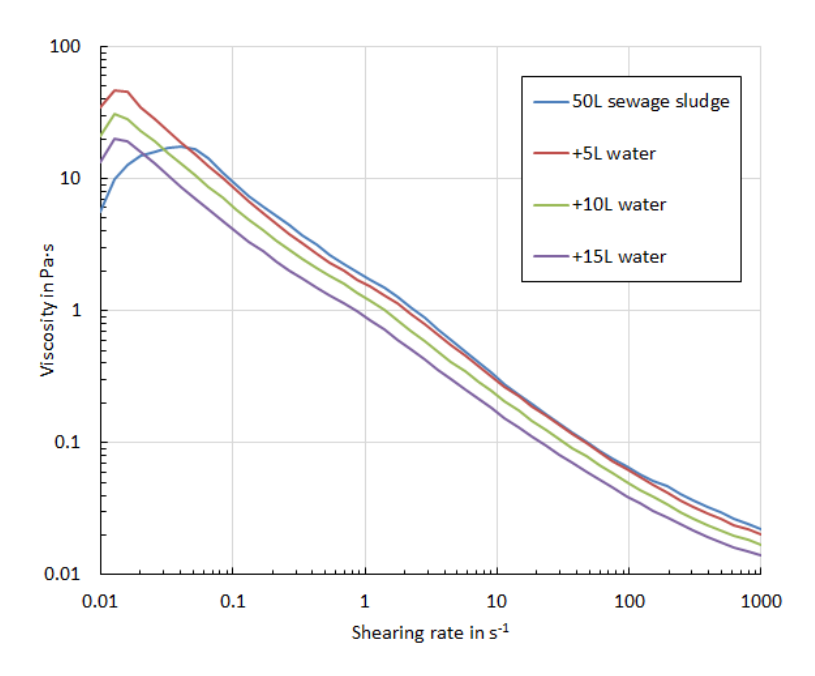


Figure 4.10: Viscosity curves for diluted sewage sludge.

### 4.4.1 Solids and elemental analysis

The sludge for these experiments was sampled in July 2019, a month later than the previous test (Section 4.3). This time the sewage treatment process was different; the iron dosing was halved, from 800 kg Fe/day to 400 kg Fe/day. This means that the vivianite formation most likely has been reduced. Table 4.4 shows the TS, VS and Fe and P concentrations for the undiluted and diluted sludge mixtures. Logically, the solids concentration (TS) decreases with increasing dilution. The differences in VS, Fe and P concentrations are most likely caused sampling and analysis inaccuracies. Samples were taken in duplicate from the top of the spiral, of which the average is shown in the table.

Sludge dilution	TS in %	VS in % of TS	Fe in mg/g ds	P in mg/g ds
0%	4.60	64.94	41.98	29.70
10%	4.33	65.05	42.83	30.17
20%	4.03	64.05	47.10	31.95
30%	3.74	63.15	42.83	29.13

Table 4.4: TS, VS and Fe and P concentrations for diluted and undiluted feed samples.

Experiments were performed with a feed rate of around 0.8 kg/s. The results are shown in Table 4.5. The sludge and solids yield to product decrease with an increasing dilution, meaning that diluted sludge is more sensitive to centrifugal forces, but also more of the solids are moved outwards. The VS content of the product flow is highest for undiluted sludge, and decreases with increasing dilution. This shows that for a more diluted sludge, the product from the spiral contains less organic material. Separation takes place between minerals and organic material, and this separation increases when diluting the sludge. Fe concentrations are highest for the product, and increase with dilution. The P concentration, however, remains similar for all outlets and dilutions. This suggests that Fe minerals other than vivianite have concentrated to the product flow, such as siderite and pyrite. These minerals were previously found by Prot et al.[39] in the magnetic product, and have densities of approximately 4 and 5 g/cm³ respectively for siderite and pyrite[23, 24].

	Sludge yield	Solids yield	TS	VS in	Fe in	P in	P recovery
	in %	in %	in %	% of TS	mg/g ds	mg/g ds	in %
			50L ur	ndiluted slu	ıdge		
Product	48	51	5.07	64.09	45.66	30.25	51
Middlings	35	33	4.48	66.91	43.12	31.19	33
Tailings	18	16	4.30	66.97	41.39	30.28	16
		1	0% dilu	ution (+5L v	water)		
Product	45	50	4.75	62.02	46.84	31.58	51
Middlings	28	27	4.02	67.40	41.19	30.24	26
Tailings	27	24	3.85	69.09	41.69	30.60	23
		2	0% dilu	tion (+10L	water)		
Product	44	49	4.52	60.64	47.66	30.73	49
Middlings	34	31	3.70	67.68	40.10	29.83	30
Tailings	23	20	3.62	67.94	42.24	32.30	21
		3	0% dilu	tion (+15L	water)		
Product	36	41	4.24	58.49	49.73	31.91	42
Middlings	26	24	3.46	67.52	40.20	29.90	23
Tailings	38	35	3.47	66.72	40.94	31.77	36

Table 4.5: Results from solids and elemental analysis of the spiral experiment with diluted sewage sludge. Feed rate of 0.8 kg/s.

Figure 4.11 shows the solids contents of the different samples. The product samples have the highest solids concentration for each mixture, while the middlings and tailings sample have similar solids concentrations per mixture. The VS content of each product is lower than the middlings and tailings, and with increasing dilution, the VS fraction decreases. It furthermore shows that the solids concentration for each flow decreases slightly with increasing dilution, which is a logical effect of dilution.

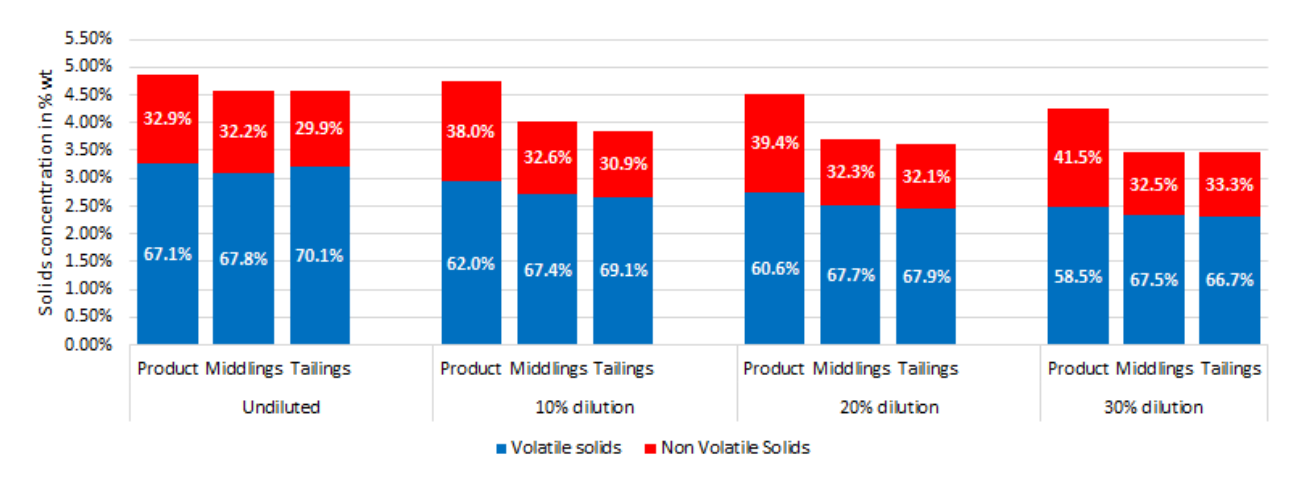


Figure 4.11: Volatile and non-volatile solids contents of the product, middlings and tailings samples for undiluted and diluted sludge. Data labels indicating the fraction of solids. Feed rate of 0.8 kg/s.

During the experiment, a slow-moving bed of sand particles was observed in the gutter directly next to the column. Part of this sand likely was a residue from experiments with synthetic sludge. An image of the sand bed can be found in the Appendix (Figure B.5). This bed was first observed with 20% diluted sludge, and also for 30% dilution. Apparently, for these dilutions the spiral is able to concentrate sand grains from sewage sludge. These particles are larger in size than vivianite and have a spherical shape, making them easier to settle and move towards the product flow.

### 4.4.2 Spiral performance

The results from the solids analysis are used to create spiral performance plots. Recoveries are expressed as recovered non-volatile solids, which include vivianite but also other minerals such as quartz, pyrite and siderite. To create the plots, multiple samples need to be taken for different splitter positions, and as ICP-OES analysis is a time-consuming method, it was decided to base these plots on non-VS content, instead of P content. As pyrite, siderite and quartz have a higher or similar density to vivianite, it is expected that if vivianite concentrates on the spiral, the other minerals will too.

Figure 4.12 shows the yield-recovery curves for the undiluted and diluted sludges, all tested with a similar feed rate. The curve for undiluted sludge is located closest to the lower limit, with the other mixtures slightly above it. No clear differences are observed between the diluted mixtures. All curves are located fairly close to the lower limit, meaning that separation has been limited.

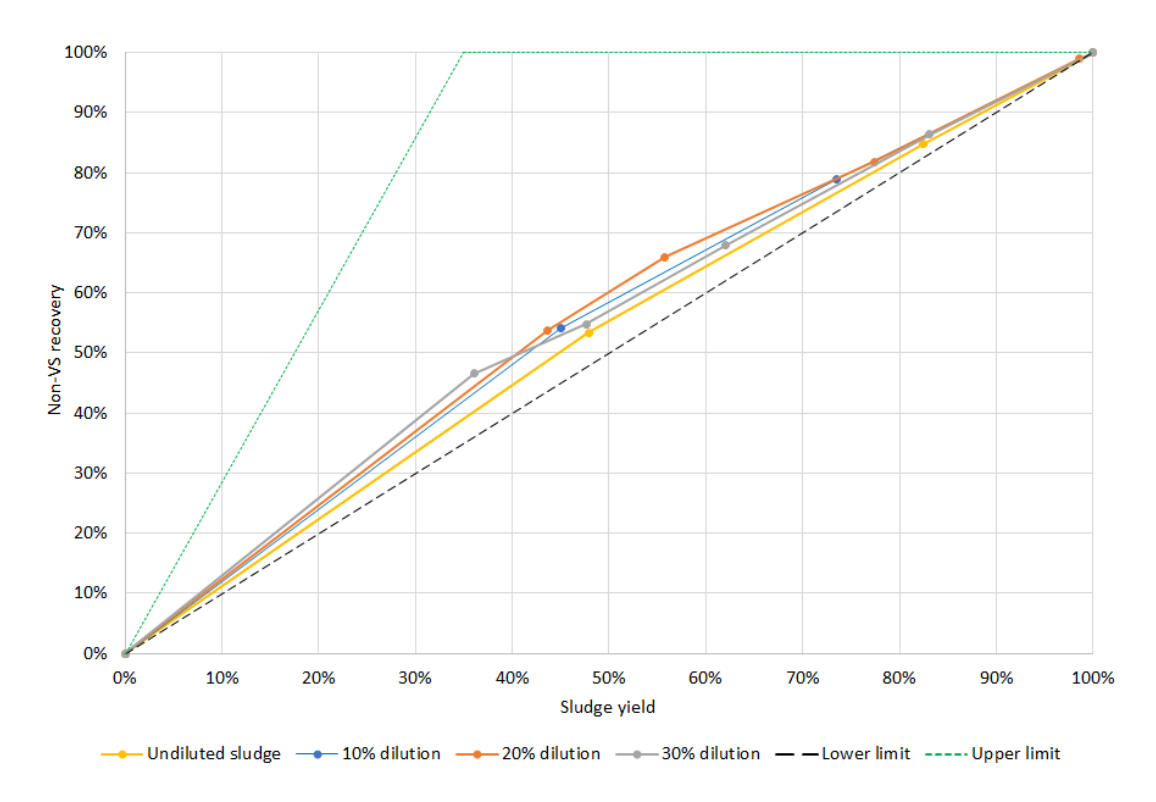


Figure 4.12: Non-VS recovery plotted against sludge yield for different diluted sludge mixtures. Feed rates around 0.8 kg/s.

A better comparison between the different dilutions can be made with Figure 4.13. The maximum efficiency is around 9% with a 40% solids yield, for the 30% diluted sludge mixture. The peak of the curve will most likely be higher than 9%, and will be located at a solids yield of 30%, which is the non-VS content (grade) of the feed. However, this point is not measured, as the minimum solids yield to product was 40% due to the minimum splitter opening. The graph shows that the efficiencies decrease with the less diluted mixtures, and the lowest efficiency is found for undiluted sludge. This clearly shows that dilution of sludge has a positive effect on the separation process on a spiral concentrator. Compared to the synthetic sludge, where an efficiency of over 80% was found, these efficiencies are relatively low.

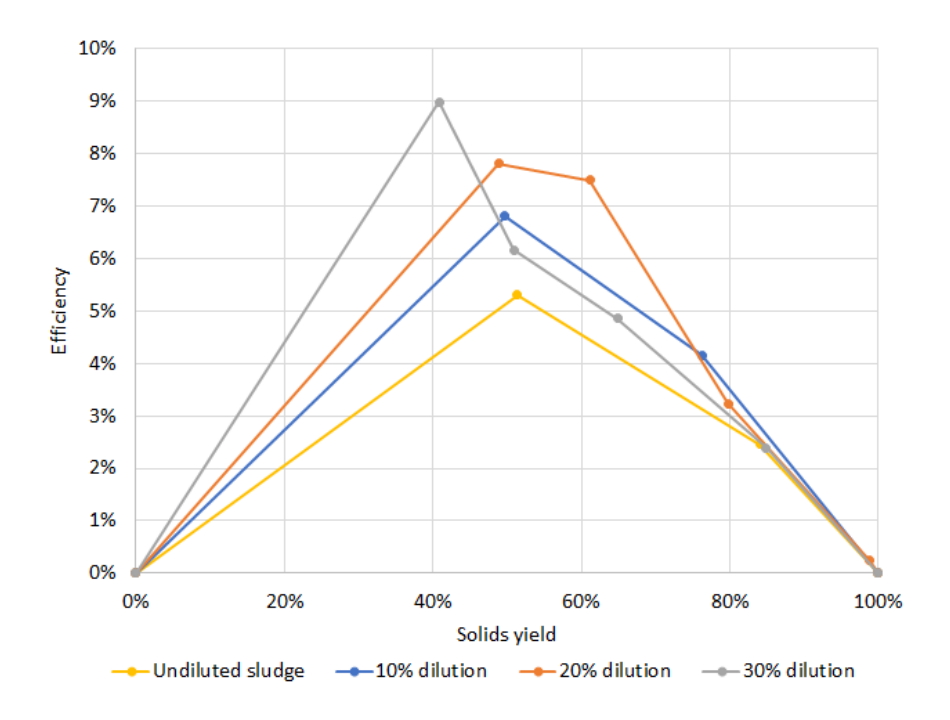


Figure 4.13: Spiral efficiency for undiluted and diluted sludge mixtures. Feed rates around 0.8 kg/s.

## 5 Discussion

This chapter discusses the results given in the previous chapter. Firstly, the reliability of the results is reviewed in Section 5.1, and the results from the centrifugal experiment and spiral experiments are discussed in Section 5.2 and Section 5.3 respectively. Finally, the financial analysis of spiral concentration of sewage sludge is given in Section 5.4, including possible applications of the vivianite product.

## 5.1 Measurement accuracy

The major inaccuracy for both the centrifuge and spiral experiments is expected in the flow rate measurements. The feed rate and the tailings flow rate of the centrifuge are measured by hand, with measuring cups and a stopwatch. The feed rate of the spiral is also measured by hand, putting a large bucket under all outlets while timing it, to determine the feed rate in g/s. Then smaller containers are simultaneously slid under each outlet, to determine the fraction of feed rate ending up in each outlet. Inaccuracies for all these measurements are expected due to human errors in time tracking.

Smaller errors are expected in the TS and VS measurements. Samples were taken in porcelain dishes. Before sampling, these dishes were stored in a desiccator and weighed. After sampling, samples were directly weighted to prevent mass loss due to chemical reactions or evaporation. Samples were then carefully dried and then stored in a desiccator. After ignition, samples were cooled in the desiccator. Masses were measured using a 4 decimal gram scale. The same scale was used to weigh the sand and PET from the synthetic sludge. During sieving of the synthetic sludge, some material might have been lost, resulting in inaccuracies.

Finally, the sample sizes could influence the reliability of the results. Samples between 100-200 g were taken during experiments with synthetic sludge. The particle sizes in the sludge were predetermined, so no outliers in size are expected, and as the pump mixes the fluid, it can be assumed that the feed is a homogeneous mixture. For synthetic sludge, the samples sizes were large enough to represent mixture well and samples taken in duplicate did not show large deviations. The sewage sludge samples, both for the centrifuge and spiral tests, were significantly smaller. Wet weights were generally 10-30 g. The sample sizes were kept small, as samples needed to be dried at room temperature, what required already a few days for these samples, and because the oven had a limited amount of space. For larger sample sizes, the analysis would have taken much more time, and it was chosen to use this time to perform more experiments. This did affect the reliability of these results. sewage sludge is a far more complex fluid than the synthetic sludge, in which particles differ strongly in type, size and shape. Larger sample sizes are required for a better sludge representation. However, samples taken in multiples generally showed comparable results in terms of TS and VS, and only a few outliers needed to be removed for further analysis. These outliers might have been caused by sampling errors, but could also be a result of an error made in the analysis. Of all sewage sludge samples that were analyzed, around 1/50 samples showed to be an outlier.

### 5.2 Centrifuge limitations and possible improvements

Compared to the theoretical recovery in the centrifuge, the results from the experiment showed different numbers. Table 4.1 shows a solids recovery of 13% and Fe and P recoveries of 33% and 23% respectively. Here a recovered particle is one that has not exited the centrifuge, so it reached the cylinder surface and stuck to it. Assuming that all P is bound in vivianite gives a vivianite recovery of 23%. Figure 4.2 shows that theoretically, if all vivianite particles are 25 µm in diameter, around 24% would be recovered. Vivianite particles in sludge are between 10 and 200 µm in diameter, so theoretically the vivianite recovery would be higher than the measured 23% over this size range. Two assumptions in the theoretically determined recovery are the shape and tortuosity factors. Both are taken at 0.5, reducing the migration velocities with 75%. This velocity reduction could in reality be higher, which would reduce the recovery. There are also several limitations in the centrifuge setup, which could have decreased the vivianite recovery.

The first inaccuracy of the centrifuge setup is the imperfection of the cylinder, meaning that it is not perfectly circular. From a fixed position next to the cylinder, the distance to the cylinder was measured while rotating it. A deviation of 0.6 mm was found, meaning that the splitter distance to the cylinder is not constant, but moves over a range of 0.6 mm when the cylinder is rotating. As the fluid film is only a few mm thick, this deviation influences the separation considerably. Another flaw of the cylinder is that the fluid flow is disturbed twice while moving down the surface. The cylinder is attached to the drill with two disks, both having 8 toes being 13 mm wide and 18 mm thick (in vertical direction), see Figure B.1 in the Appendix. The cylinder is connected to these toes, meaning that the fluid flow is disturbed twice for 18 mm long.

If the film partially remixes when it crosses the toes, the effective residence time, meaning the time that particles migrate radially, decreases. Theoretically, the film thickness would be 2.25 mm for a feed rate of 1.17 L/s that was used during experiments. However, the thickness during experiments was measured to be just over 1 mm. The difference between the theoretical thickness and measured thickness could be caused by the flow disturbance. When the flow reaches the toes, it bounces off the cylinder face and possibly directly exits the cylinder without settling again on the face, reducing the amount of sludge on the cylinder face and thereby the film thickness. Another explanation for the smaller film thickness could be the shear-thinning behaviour of the sludge, reducing the viscosity and thereby decreasing the film thickness. As previously shown in Figure 3.1, the viscosity of sludge is a function of shear rate. With increasing shear rate, particles in fluids orientate in one direction which decreases the viscosity. If shearing rates in reality are higher in the centrifuge than theoretically estimated, then the sludge would have a lower viscosity, meaning a thinner film in the cylinder.

The centrifuge did not function in the way it was meant to. The goal was to create a flow where heavy particles were concentrated (product), which would then be separated from the rest of the flow (tailings) with a splitter. Product and tailings samples did not show significant differences, but it was observed that feed samples contained more solids and a higher Fe and P concentration that sludge exiting the centrifuge, suggesting that vivianite stayed in the cylinder without escaping. This would be caused by friction between the surface and the minerals, preventing them to move downwards. Two adjustments are possible to let the minerals escape the system:

- Decrease the rotational velocity of the cylinder. The centrifugal force then decreases, reducing
  the friction along the cylinder surface. By reducing the rotational velocity, terminal velocities of
  particles also decrease. To achieve the same radial migration, the cylinder needs to be longer.
- Change the shape of the cylinder into a cone with the larger diameter at the bottom. The centrifugal force is then no longer directed perpendicular on the cylinder surface but at a smaller angle, actually forcing the particles to move out of the system. This way the flow behaviour and film thickness will change too.

### 5.3 Spiral concentration for vivianite recovery

The following sections discuss the results obtained from experiments with the spiral concentrator. Section 5.3.1 discusses the results obtained from tests with synthetic sludge, and to what extent the synthetic sludge represents the sewage sludge. Section 5.3.2 and Section 5.3.3 discuss the experiments with undiluted and diluted sewage sludge.

### 5.3.1 Synthetic sludge

The results in Section 4.2 show that the separation mechanism works well with synthetic sludge. It shows recoveries op to 90% with a grade of almost 78%. The recoveries and grades increase when the feed grade increases. Next to that, the fluid yield decreases when increasing the flow rate. This is beneficial, as less fluid needs to be processed after spiral concentration. Ideally, one would want to capture as much sand as possible but yield the least possible amount of fluid. The maximum rate was set at 1.57 kg/s, but possibly the performance of the spiral could be even better for a higher feed rate. The solids of the product consisted of 22.3-43.9% of PET. This could be partially caused by the repulper halfway the spiral. Here a part of the middlings flow is forced to move towards the column into the gutter, and if this flow contained PET, it will end up in the product outlet. Up to 90.4% of sand was recovered, with the remaining 4.5% in the middlings and 5.1% in the tailings outlet. These were most likely smaller grains that were still in transport or unable to move inwards due to high centrifugal forces. It was observed that with increasing feed rate, the sand recovery in the tailings increases.

The synthetic sludge was used to mimic the behaviour of particles in sewage sludge. While the densities of sand and PET are similar to vivianite and organics in sewage sludge, is does not mimic sewage sludge accurately. In synthetic sludge, particles are able to move individually, while in sewage sludge vivianite often is present in an organic matrix. The shape of sand and PET also does not represent organic particles and vivianite well. Finally, the viscosity of synthetic sludge was significantly lower than the sewage sludge viscosity, as shown in Figure A.1.

#### 5.3.2 Digested sewage sludge

Compared to the synthetic sludge, more % of the sewage sludge was captured in the product outlet. For a feed rate of 1.2 kg/s, this yield was 22% for synthetic sludge compared to a 36% yield for sewage sludge. As the synthetic sludge has a lower viscosity, it is more sensitive to the centrifugal forces and easily moves towards the outer rim, while sewage sludge was more prone to move towards the inner column. This can be seen in Figure 5.1, where both fluids flows are shown when entering the spiral. Synthetic sludge does not enter the gutter near the column, while sewage sludge immediately flows into it. The fluid remains in the gutter until it reaches the product outlet, and this causes the sewage sludge to have a higher fluid yield to product.





Figure 5.1: Synthetic sludge (A) and sewage sludge (B) entering the spiral. Red circles indicate the different flow behaviours.

The solids analysis did not show an effective separation between volatile and non-volatile solids. The solids concentration in the product outlet was generally higher than in the middlings and tailings outlets, but differences were small. The volatile solids content was around 70% for all samples. Also looking at the elemental compositions of the samples, no clear differences are observed in Fe and P concentration.

Samples taken before the repulper did show a clear difference in TS content, with almost 10% in the product flow, 4.67% in the middlings and 2.66% in the tailings flow. For the product flow, the TS content more than doubled compared to the feed. This means that before the sludge reaches the repulper, solids are concentrated towards the column. The repulper clearly harmed the concentration process of the spiral, as at the bottom of the spiral, solids concentration of all outlets were similar. Flow rates per outlet could not be measured before the repulper, so sludge or solids yields are not determined. To prevent the negative effect of the repulper in future experiments, it was removed from the spiral.

The spiral without the repulper was then again tested with sewage sludge. The results from tests with and without the repulper are compared in Table 5.1. The largest difference is in the sludge and solids yield to product. With the repulper, much more material is forced towards the product outlet. The cause of this is previously explained in Section 4.3.2. The difference in TS between product and tailings is larger for the experiments without the repulper. Also relatively more Fe was concentrated in the product without the repulper. The VS, Fe and P contents of the samples taken without the repulper are lower, but this is because it was tested with a sludge sampled on a different day. The feed of the sludge tested with the repulper had a TS of 4.86% and a VS of 67.82%, while the sludge tested without the repulper were also slightly lower.

Table 5.1: Results of spiral experiments with undiluted sludge, with and without the repulper. Feed rates of 0.9 kg/s.

	Sludge yield in %	Solids yield in %	TS in %	VS in %	Fe in mg/g	P in mg/g	P recovery
Draduat			111 70	of TS	ds	ds	in %
Draduat			\	Nith repulp	er		
Product	63	64	4.87	67.13	46.67	31.49	64
Middlings	36	35	4.57	67.75	44.92	32.20	36
Tailings	1	1	4.58	70.08	45.67	32.60	1
-			W	ithout repu	lper		
Product	48	51	5.07	64.09	45.66	30.25	51
Middlings	35	33	4.48	66.91	43.12	31.19	33
Tailings							

It was previously observed that in the third turn of the spiral, the solids concentration in the product flow was around 10%, more than double the concentration of the feed. However, at the bottom of the spiral the TS was only around 4.9%. It was thought that this difference was caused by the repulper halfway down the spiral. However, the experiment without the repulper shows a TS much lower than 10% in the product outlet, so there is another factor decreasing the product solids concentration. One reason could the shape of the trough. A gutter is present near the column, where a large portion of the sludge flows into and then is unable to escape it. Further down the spiral, more sludge has entered the gutter, meaning more fluid and therefore lowering the solids concentration. The 10% solids concentration in the third turn shows that solids do migrate towards the column, but at the bottom of the spiral, too much fluid has entered the gutter which decreased the solids concentration of the final product. This could be prevented by changing the shape of the spiral trough. If the gutter is removed, solids will still concentrate towards the column, but fluid is able to move away from the column again. This could result in a highly concentrated product flow.

### 5.3.3 Effect of diluting sewage sludge

An additional test was performed with sludge diluted with water, to lower the sludge viscosity and investigate the influence of this on the separation process. The results of the diluted sludge mixtures show that an increase in dilution improves the separation process of volatile and non-volatile solids on the spiral, and solids concentration towards the product flow increases. The spiral efficiency is still low, even for a 30% dilution. A large fraction of the solids still end up in the middlings or tailings, and the TS of the product has only increased about 0.5% compared to the feed. Separation of organic material and minerals did take place to some extent, but is still relatively small compared to the sand and PET in synthetic sludge. Elemental analysis showed an increase in Fe concentration with dilution, while the P concentrations were similar for all outlets and dilutions. Fe minerals other than vivianite have concentrated on the spiral, which are most likely pyrite and siderite, having higher densities than vivianite and were also found in the magnetically recovered product by Prot et al.[39]. It is expected that if the sludge is diluted more, the concentration and separation of organics and minerals on the spiral will increase.

Further dilution, however, is undesired. Diluting sludge will increase the total sludge volume, meaning that a higher spiral capacity is needed. The sludge also needs to be dewatered afterwards, meaning that the dewatering costs will increase if sludge is diluted. The results show that when sludge is diluted, the sludge yield to product decreases. For a 30% dilution, the sludge yield was 36%, compared to 48% for undiluted sludge. The sludge volume increased with a factor 1.3, so the yield should have this ratio too if compared to the undiluted sludge of 50 L. This results in a sludge yield of 46.8% for a 30% dilution, almost as high as for undiluted sludge. The same holds for the other dilutions, which show that an increase in sludge dilution does not decrease the sludge yield to product, but it remains more or less equal. For spiral concentration of sewage sludge, the grade of the product is of less importance than the vivianite recovery, as the product will be processed by magnetic separation, which will increase the product grade significantly. Preferably, the product flow would have a solids concentration as high as possible, with the majority of the vivianite recovered. The capacity for the magnetic separator is then decreased, and the vivianite can be separated magnetically from the other solids.

A promising phenomenon was observed during experiments with 20% diluted sludge. A slow-moving bed of sand particles was seen near the spiral column (Figure B.5), suggesting that sand particles had concentrated on the spiral. This sand was a residue from experiments with synthetic sludge. Sand particles are spherical and generally larger than the vivianite minerals, and therefore are concentrated easier towards the column. Diluting sewage sludge has improved the concentration of sand and iron minerals on the spiral, but did not induce vivianite concentration.

## 5.4 Financial analysis

The purpose of pre-concentration of vivianite by spiral concentration is to reduce the total processing costs for vivianite recovery, as the current technique by magnetic separation is relatively expensive. In this section, the cost reduction is estimated for when sludge is pre-concentrated with a spiral concentrator.

The STP in Nieuwveer, where a magnetic separation pilot plant was tested, produces around 144,000 m³ of sludge per year[48], so just over 16 m³ per hour. An Outotec SLon 750 was used in the pilot plant, having a capacity of 1 m³/hour. If sludge was processed three times with the magnetic separator, vivianite recoveries of 69% were measured with a grade of 70%. A single-pass process showed to be insufficient, as only 25% was recovered with a grade of 71%[48]. As sludge needs to pass the separator three times, the yearly capacity of the separator is three times the sludge production at Nieuwveer, so almost 50 m³/hour. The CAPEX of a full-scale processing plant to be installed at Nieuwveer, including pumps and settling tanks, was estimated to be €500,000, with an OPEX of €100,000[48].

Table 5.2 shows that the costs of a SLon magnetic separator increase linearly with its required capacity. Outotec offers multiple SLon types ranging in size and capacity, their price is assumed to be €6000 per hourly processed ton of sludge[38]. This number is determined for SLon separators treating ore, so the costs might differ for a specially developed separator for sewage sludge treatment. A single spiral costs €5446 and can handle a capacity of 3.6 m³/hour, assuming a feed rate of 1 L/s. Five spirals would be required to process sewage sludge from the Nieuwveer STP. The yield to product of the spiral is 40-50%, so this would mean a capacity and cost reduction of 50-60% for the SLon magnetic separator if the magnetic separator only processes the spiral product. The additional costs of pre-concentration are the CAPEX of the spirals, pumps for the spirals and some spiral maintenance costs.

Table 5.2: Costs for a SLon magnetic separator[38, 48] and a Multotec MX7 spiral.

	SLon magnetic separator	Multotec MX7 spiral
CAPEX Electricity costs Consumables (e.g rod matrices)	€6000 /ton sludge /hour €0.10 /m³ sludge €0.04 /ton sludge	€ 5,446 - -

It is unknown if the magnetic separator would perform better when processing pre-concentrated sludge. The magnetic vivianite recovery for sludge from the digester is 69% with a grade of 70%, but might improve for a more concentrated input. When vivianite is recovered, revenue is made from selling vivianite concentrate, but costs are also reduced concerning sludge disposal. Because vivianite is removed from sludge, the sludge volume that needs to be disposed of is reduced. However, there are also extra costs concerning sludge dewatering. For sludge dewatering, polymers are used to coagulate solids and produce flocs. As the tailings from the density and magnetic separators have lower solids concentrations, more polymers are needed to dewater it, and therefore the dewatering costs increase. Tailings sludge from the magnetic separator required 20% more polymers to dewater, compared to the feed[48]. The polymer increase for spiral tailings dewatering will need to be determined experimentally.

Results from the spiral experiments have shown limited solids and P concentration. If vivianite can be concentrated by density concentration at some point, either by an adjusted spiral or other types of density concentrators, this concentrator could be used for pre-concentration. This concentrator could then directly process the sewage sludge on site at an STP. There are two options for the industrial

application of magnetic vivianite recovery. The first option is to let each STP operate its own low-capacity SLon separator. The disadvantage is that this requires an extra investment from the STP, and the STP is responsible for the sale of the vivianite concentrate. Another disadvantage is that sludge production varies seasonally, so the maximum capacity of the SLon is not used all year round. The second option is to let STPs transport the spiral product to a central location, where a high-capacity SLon processes sludge coming from different STPs. This could be an independent vivianite recovery plant, which is responsible for the sale of the vivianite concentrate. The disadvantage here is the transport cost of sludge to this plant. The Netherlands has 352 STPs, of which many are clustered, as can be seen in Figure B.6. Several magnetic vivianite recovery plants could be installed throughout the country, for example for each water board, all processing sludge from surrounding STPs.

The vivianite product could be used directly for fertilizer production. Studies have shown that vivianite as a fertilizer has a four to six times higher efficiency than calcium phosphate. It furthermore improves the production of corn and beans and reduces Fe chlorosis of grapevines and strawberries[64]. Chlorosis is a deficiency in iron common in calcareous soil crops, which could lead to crop death. Another option to use vivianite as a fertilizer, is to dissolve the mineral in potassium hydroxide, resulting in a liquid  $K_3PO_4$  which can be used as a fertilizer, and  $Fe(OH)_2$  which can be precipitated as  $FeCl_3$  with HCl. Vivianite could also be used as a pigment for paint, this application can be traced back to the Middle Ages[66]. Finally, vivianite is applicable in lithium-ion battery production. Vivianite is used for the production of lithium iron phosphate (LiFePO<sub>4</sub>), which is increasingly used for Li-ion battery production[64].

## 6 Conclusion

The goal of this research was to investigate the feasibility of vivianite recovery by density concentration with a spiral concentrator. Spiral concentration could then be used as a pre-concentration step before vivianite recovery by magnetic separation, which would reduce the magnetic processing costs. The research question was formulated as follows:

• Can spiral concentration be used for concentration of vivianite in digested sewage sludge?

The answer to this question is found by reviewing literature on spiral concentration principles and by performing laboratory experiments. Additionally, the theoretical cost reduction of using spiral concentration as a pre-concentration step is estimated.

The high viscosity of sewage sludge complicates the separation mechanism on a spiral concentrator. The sludge shows strong shear-thinning behaviour, and the viscosity decreases with increasing temperature. A centrifugal experiment was designed and tested to investigate vivianite migration in sludge under a G-force of 245. A thin fluid film was split at the bottom of a rotating cylinder, in which heavier particles are forced towards the cylinder surface by centrifugal forces. A 13% decrease in solids concentration and a 33% and 23% decrease in Fe and P content respectively was found for material exiting the cylinder, compared to the feed. Hypothesized is that vivianite and other heavy minerals have migrated towards the cylinder surface, but were unable to exit the system due to high friction forces along the cylinder surface, and got stuck in the system. This hypothesis has not been proven to be true, but theoretical computations also suggest that the particles should migrate towards the surface under these conditions. Due to time limitations and limitations in the setup, no further experiments were performed with this setup.

Spiral experiments with synthetic sludge, a water-glycerol mixture with sand and PET, showed an effective separation of sand and PET with sand recoveries up to 90% and grades up to 78%. The synthetic sludge had a zero shear viscosity of 0.025 Pa·s, 25 times higher than water. The spherical and flaky shapes of sand and PET particles respectively induced an effective separation, but were not a realistic representation of particles in sewage sludge. The first tests with sewage sludge showed a product solids concentration and phosphorus content that was similar to the feed, so no effective separation took place. A remixer located in the fourth turn of the spiral, which negatively influenced the separation process, was removed from the spiral afterwards.

Additional experiments were performed with sewage sludge which was diluted with water, to lower the viscosity. The viscosities of the diluted mixtures were measured, showing that the viscosity decreases linearly with dilution, a 20-30% viscosity reduction with 10% dilution. The fluid flow on the spiral changed significantly with dilution. Where the fluid yield to product was 48% for undiluted sludge, it was 36% for 30% diluted sludge. The Reynolds number increases with decreasing viscosity, resulting in a more turbulent flow. This turbulence increased the grade of the product. The volatile solids content for the 30% diluted sludge was 58.5%, while this was 64.1% for undiluted sludge. While diluting the sludge improved the separation process between organic material and minerals, spiral efficiencies were relatively low, 9% compared to 80% for synthetic sludge. This number was based on recovered non-volatile solids. ICP-OES analysis showed that the Fe concentrations were highest for the product outlet, with the highest concentration for the most diluted mixture. The P concentrations, however, were similar for all outlets and dilutions, suggesting that only Fe minerals other than vivianite, such as pyrite and siderite, concentrated in the product flow. Also sand grains were concentrated after a dilution of 20%. These grains were observed as a slow-moving bed near the column. The experiments showed that sand grains and iron minerals other than vivianite can be concentrated on a

spiral, however with low efficiencies. Vivianite has not been concentrated during these experiments, which was the target mineral of this research.

One factor limiting the concentration mechanism of the spiral, is its trough shape. A gutter near the column captures a large fraction of the fluid flow, which is then unable to escape from the gutter. This gutter reduced the product grade and solids concentrations significantly. Undiluted sludge samples taken from the third turn on the spiral showed a solids concentration of 10% in the product flow, more than twice the concentration of the feed, which was not observed at the bottom of the spiral. In the third turn of the spiral, the flow fraction in the gutter is still small, but increases throughout the spiral, meaning that the grade and solids concentration of the product decreases throughout the spiral. This can be solved by changing the shape of the spiral trough or reducing the spiral length. Spiral concentration has the potential to concentrate vivianite from sewage sludge, but improvements are necessary to increase the separation efficiencies.

Financial analysis showed that the processing costs for magnetic separation are directly related to the capacity of the machinery, based on numbers of Outotec. Spiral concentration could significantly reduce the required capacity for magnetic separation. Sludge yields to product on the spiral were 40-50%, reducing the capacity for magnetic separation with 50-60%. Sludge disposal costs will decrease after vivianite recovery, as the total sludge volume will decrease when vivianite is removed. Additional costs of pre-concentration with a spiral are the price of the spiral itself and pumps and maintenance costs for the spiral. It is furthermore expected that sludge dewatering costs will increase. Spiral and magnetic concentrators could be installed on each STP for vivianite recovery. Alternatively, the magnetic recovery could take place on a different site by an independent recovery plant. This high capacity plant could process pre-concentrated sludge from multiple STPs. The vivianite product can be sold by a single provider for fertilizer production, or other applications such as paint pigment or for lithium-ion battery production. Before vivianite recovery systems can be developed, improvements in spiral concentration are necessary to increase the vivianite recovery. Recommendations for future research for improved vivianite recovery are given in the next chapter.

## 7 Recommendations

For the thin-film centrifuge to properly function, some adjustments are required. To ensure that the cylinder has no deviations and the film is not disturbed while flowing through the cylinder, it should not be attached to a drill from inside, but fixed between rotating wheels on the outside. The wheels generate the rotation of the cylinder, but also keep it firmly in place to reduce the splitter deviation. The inside of the cylinder is then empty, so the flowing film will not be disturbed. To avoid minerals being stuck in the system, the radius of the cylinder should be slightly larger at the bottom, so changing the cylinder to a conical shape.

Vivianite recovery by spiral concentration could be increased by several adjustments. This research showed that diluting the sludge improves the separation mechanism, but is an undesired option as it will increase the total volume to be processed, and will increase dewatering costs. For future research, different spirals could be used which do not have a gutter near the column, which was present in the MX7 coal spiral. A steeper primary slope and flatter trough slope could also improve the vivianite recovery, as sludge will experience higher centrifugal forces and less secondary gravitational force towards the column. Some additional experiments could be performed on the MX7 spiral. To investigate how the product flow changes along the spiral, samples could be taken from each turn on the spiral. In this research, only one sample was taken from the third turn and the rest from the bottom of the spiral. Additionally, magnetic foil could be added on the trough surface. This would increase the downwards directed force on vivianite particles, increasing their settling velocity and possibly improving the recovery.

One difficulty in this research was to determine the exact vivianite concentration. A combination of solids analysis and elemental analysis was used to make an estimation. However, further research for vivianite characterization with for example SEM-EDX, XRD and Mössbauer spectroscopy is recommended. Additional research on vivianite growth in sewage sludge could also be beneficial for increasing recoveries. The crystals could grow larger if the solid retention time is increased in the digestion process[58]. Larger crystals would be easier to separate both with the spiral concentrator and magnetic separator. In this research sludge from only one source has been tested, but a comparison between different sludge sources is recommended for future research.

Finally, if higher recoveries with spiral concentration can be achieved, it should be investigated how this would influence the recoveries in magnetic separators. Then it could also be investigated if recirculation of middlings in the spiral would improve the vivianite recovery. A study on the dewaterability of the spiral tailings is also recommended. A more extensive financial analysis should also be performed, including possible market prices for the vivianite product, but also better estimations on processing costs. This should be done in cooperation with industrial partners delivering the separators, as the processing equipment will most likely be tailor-made for vivianite recovery.

- [1] J.R.L. Allen. Chapter 2 entrainment and transport of sedimentary particles. In J.R.L. Allen, editor, *Sedimentary Structures Their Character and Physical Basis Volume I*, volume 30 of *Developments in Sedimentology*, pages 57 110. Elsevier, 1982.
- [2] APHA, AWWA, WEF. Standard methods for the examination of water and wastewater. American Public Health Association, Washington DC, 20th edition, 1998.
- [3] Y. Atasoy and D.J. Spottiswood. A study of particle separation in a spiral concentrator. *Minerals Engineering*, 8(10):1197 1208, 1995.
- [4] R.A. Bagnold. Experiments on gravity-free dispersion of large solid spheres in a Newtonian fluid under shear. *Proceedings of The Royal Society A: Mathematical, Physical and Engineering Sciences*, 225:49–63, 1954.
- [5] S. Bentov, E.D. Aflalo, J. Tynyakov, L. Glazer, and A. Sagi. Calcium phosphate mineralization is widely applied in crustacean mandibles. *Scientific reports*, 6, 22118, 2016.
- [6] J.S. Browning. Mica benefication. U.S. Bureau of Mines Bull., 622:21 pp, 1973.
- [7] R.O. Burt. Gravity concentration technology, volume 5. Elsevier, Amsterdam, 1984.
- [8] D. Cordell and S. White. Sustainable phosphorus measures: Strategies and technologies for achieving phosphorus security. Agronomy, 3:86–116, 03 2013.
- [9] N Cullen, R Baur, and P Schauer. Three years of operation of North America's first nutrient recovery facility. *Water science and technology: a journal of the International Association on Water Pollution Research*, 68:763–8, 2013.
- [10] R. Dallaire, A.R. Laplante, and J. Elbrond. Humphrey's spiral tolerance to feed variations. *Bull. Cann. Inst. Min. & Metall.*, 71:128–134, 08 1978.
- [11] Z.T. Deng. Experimental investigation of particle flow in a spiral concentrator. Master's thesis, McGill University, 2015.
- [12] J. Drzymala. *Mineral processing: foundations of theory and practice of minerallurgy*. Oficyna Wydawnicza PWr., Wroclaw, 2007.
- [13] E. Frossard, J.P. Bauer, and F. Lothe. Evidence of vivianite in feso4-flocculated sludges. *Water Research*, 31(10):2449 2454, 1997.
- [14] H.J. Glass, N.J. Minekus, and W.L. Dalmijn. Mechanics of coal spirals. *Minerals Engineering*, 12(3):271 280, 1999.
- [15] W Gleason. An introduction to phosphorus: History, production, and application. *JOM*, 59(6): 17–19, 2007.
- [16] G.W. Gleeson. Why the Humphreys spiral works. *Engineering and Mining Journal*, 146:85 86, 1945.
- [17] M.J. Glimcher. Bone: Nature of the Calcium Phoshpate Crystals and Cellular, Structural, and Physical Chemical Mechanisms in Their Formation. *Reviews in Mineralogy and Geochemistry*, 64(1):223–282, 2006.

[18] K.N. Han and W.C. Say. On the separation of fine particles by centrifugation. *International Journal of Mineral Processing*, 14(4):265 – 273, 1985.

- [19] A.B. Holland-Batt. Spiral separation: theory and simulation. *Trans. Instn. Min. Metall.* (Sect. C: Mineral Process. Extr. Metall.), 98:46–60, 1989.
- [20] A.B. Holland-Batt. Some design considerations for spiral separators. *Minerals Engineering*, 8 (11):1381 1395, 1995.
- [21] A.B. Holland-Batt and P.N. Holtham. Particle and fluid motion on spiral separators. *Minerals Engineering*, 4(3):457 482, 1991.
- [22] R.Q. Honaker, M. Jain, B.K. Parekh, and M. Saracoglu. Ultrafine coal cleaning using spiral concentrators. *Minerals Engineering*, 20(14):1315 1319, 2007.
- [23] Hudson Institute of Mineralogy and mindat.org. Physical properties of pyrite, Accessed: 22-07-2019. URL https://www.mindat.org/min-3314.html.
- [24] Hudson Institute of Mineralogy and mindat.org. Physical properties of siderite, Accessed: 22-07-2019. URL https://www.mindat.org/min-3647.html.
- [25] P.V. Iyer. Magnetic and electrostatic separation. In P. Darling, editor, *SME Mining Engineering Handbook*, chapter 14.6, pages 1533–1545. Society for Mining, Metallurgy, and Exploration, Inc., USA, 3rd edition, 2011.
- [26] P.K. Jain and V. Rayasam. An analytical approach to explain the generation of secondary circulation in spiral concentrators. *Powder Technology*, 308:165 177, 2017.
- [27] P.C. Kapur and T.P. Meloy. Spirals observed. *International Journal of Mineral Processing*, 53(1): 15 28, 1998. Particle Science and Technology in the 21st Century.
- [28] P.C Kapur and T.P Meloy. Industrial modeling of spirals for optimal configuration and design: spiral geometry, fluid flow and forces on particles. *Powder Technology*, 102(3):244 252, 1999.
- [29] A. Kelessidis and A.S. Stasinakis. Comparative study of the methods used for treatment and final disposal of sewage sludge in European countries. Waste Management, 32(6):1186 – 1195, 2012.
- [30] B.V. Kizevalter. Theoretical fundamentals of gravity concentration processes. *Nedra Press. Moscow*, page 295 pp, 1979.
- [31] L. Korving, M.C.M. van Loosdrecht, and P. Wilfert. Effect of iron on phosphate recovery from sewage sludge. *Phosphorus Recovery and Recycling*, pages 303–326, 2019.
- [32] H.H. Luesink, D.F. Broens, M.A. van Galen, F.E. de Buisonjé, and E. Georgiev. Terugwinning van fosfaat; Economische verkenning van kansen en mogelijkheden. Technical report, LEI Wageningen UR, 2013.
- [33] R.D. MacNicol and P.H.T. Beckett. The distribution of heavy metals between the principal components of digested sewage sludge. *Water Research*, 23(2):199 206, 1989.
- [34] L. Moss, J.F. Donovan, S. Carr, L. Stone, C. Polo, W. Khunjar, R. Latimer, S. Jeyanayagam, N. Beecher, and L. McFadden. Enabling the future: Advancing resource recovery from biosolids. Technical report, Water Environment Federation, 2013.
- [35] Multotec. Coal spiral concentrators, Accessed: 07-08-2019. URL https://www.multotec.com/public/uploads/fileLibrary/73661%20Multotec%20Coal%20Spiral%20Concentrators%20Bro-Digital-3a18c.pdf.

[36] Normensand GmbH. CEN-Standard Sand according to EN 196-1, 2019. URL https://www.normensand.de/en/products/cen-standard-sand-en-196-1/. Accessed: 09-05-2019.

- [37] O. Nowak, S Keil, and C. Fimml. Examples of energy self-sufficient municipal nutrient removal plants. *Water science and technology: a journal of the International Association on Water Pollution Research*, 64:1–6, 2011.
- [38] Outotec. Slon VPHGMS iron ore beneficiation product line, 2017.
- [39] T. Prot, V.H. Nguyen, P. Wilfert, A.I. Dugulan, K. Goubitz, D.J. De Ridder, L. Korving, P. Rem, A. Bouderbala, G.J. Witkamp, and M.C.M. van Loosdrecht. Magnetic separation and characterization of vivianite from digested sewage sludge. *Separation and Purification Technology*, 224: 564 579, 2019.
- [40] R.G. Richards, D.M. MacHunter, P.J. Gates, and M.K. Palmer. Gravity separation of ultra-fine (-0.1mm) minerals using spiral separators. *Minerals Engineering*, 13(1):65 77, 2000.
- [41] R.H.P. Ringeling, H.J. Glass, and M. Olijve. Optimizing soil remediation with coal spirals. *Proceedings 4th Conference on Environment and Mineral Processing*, pages 295–300, 1998.
- [42] O.F. Schoumans, J. Willems, and G. van Duinhoven. 30 vragen en antwoorden over fosfaat in relatie tot landbouw en milieu. Alterra, Wageningen, 2008.
- [43] O.F. Schoumans, F. Bouraoui, C. Kabbe, O. Oenema, and K.C. van Dijk. Phosphorus management in Europe in a changing world. *AMBIO*, 44(2):180–192, 2015.
- [44] M.A. Seitz, R.J Riedner, S.K. Malhotra, and R.J. Kipp. Iron-phosphate compound identification in sewage sludge residue. *Environmental Science & Technology*, 7, 1973.
- [45] D.B. Simons and F. Sentürk. *Sediment Transport Technology: Water and Sediment Dynamics*. Water Resources Publications, Littleton, Colorado, 1992. ISBN 0-918334-66-7.
- [46] R. Sivamohan and E. Forssberg. Principles of spiral concentration. *International Journal of Mineral Processing*, 15(3):173 181, 1985.
- [47] N. Subasinghe. Gravity concentration and heavy medium separation. In P. Darling, editor, *SME Mining Engineering Handbook*, chapter 14.4, pages 1533–1545. Society for Mining, Metallurgy, and Exploration, Inc., USA, 3 edition, 2011.
- [48] G. Sudintas. Vivianite extraction from digested sewage sludge utilizing a magnetic separator. Graduation report, Avans University of Applied Sciences, 2019.
- [49] D.G. Thomas. Transport characteristics of suspension: VIII. a note on the viscosity of Newtonian suspensions of uniform spherical particles. *Journal of Colloid Science*, 20(3):267 277, 1965.
- [50] S.K. Tripathy and Y. R. Murthy. Modeling and optimization of spiral concentrator for separation of ultrafine chromite. *Powder Technology*, 221:387 394, 2012.
- [51] K.C. van Dijk, J.P. Lesschen, and O. Oenema. Phosphorus flows and balances of the European Union member states. *Science of The Total Environment*, 542:1078 1093, 2016.
- [52] Ministerie van Infrastructuur en Milieu. Inzameling, transport en behandeling van afvalwater in Nederland, 2014.
- [53] M.K.G. Vermaak, H.J. Visser, J.B. Bosnian, and G Krebs. A simple process control model for spiral concentrators. *Journal of the Southern African Institute of Mining and Metallurgy*, 108: 147–154, 2008.

[54] A. Volk. Calculate density and viscosity of glycerol/water mixtures, Accessed: 13-02-2019. URL http://www.met.reading.ac.uk/~sws04cdw/viscosity calc.html.

- [55] D.P. Van Vuuren, A.F. Bouwman, and A.H.W. Beusen. Phosphorus demand for the 1970–2100 period: A scenario analysis of resource depletion. *Global Environmental Change*, 20(3):428 439, 2010.
- [56] P. Wei, Q. Tan, W. Uijttewaal, J.B. van Lier, and M. de Kreuk. Experimental and mathematical characterisation of the rheological instability of concentrated waste activated sludge subject to anaerobic digestion. *Chemical Engineering Journal*, 349:318 326, 2018.
- [57] F. Westheimer. Why nature chose phosphates. Science, 235 (4793):1173–1178, 1987.
- [58] P. Wilfert. Phosphate Recovery From Sewage Sludge Containing Iron Phosphate. PhD thesis, Delft University of Technology, 2018. doi: 10.4233/uuid: f3729790-0cfe-4f92-866b-eca3f2f2df24.
- [59] P. Wilfert, P.S. Kumar, L. Korving, G.J. Witkamp, and M.C.M. van Loosdrecht. The relevance of phosphorus and iron chemistry to the recovery of phosphorus from wastewater: A review. *Environmental science & technology*, 49, 2015.
- [60] P. Wilfert, A. Mandalidis, I. Dugulan, K. Goubitz, L. Korving, H. Temmink, G.J. Witkamp, and M.C.M. van Loosdrecht. Vivianite as an important iron phosphate precipitate in sewage treatment plants. *Water research*, 104:449–460, 2016.
- [61] P. Wilfert, L. Korving, P.C. Rem, G.J. Witkamp, M.C.M. van Loosdrecht, I. Dugulan, and K. Goubitz. Method and system for phosphate recovery from a stream. Patent: nl 2018525, 2017.
- [62] P. Wilfert, L. Korving, I. Dugulan, K. Goubitz, G.J. Witkamp, and M.C.M. van Loosdrecht. Vivianite as a key mineral in sewage treatment plants with potential for phosphate recovery. *Submitted to: Water Research*, 2018.
- [63] B.A. Wills and J.A. Finch. Chapter 10 gravity concentration. In B.A. Wills and J.A. Finch, editors, *Wills' Mineral Processing Technology (Eighth Edition)*, pages 223 244. Butterworth-Heinemann, Boston, 8th edition, 2016.
- [64] Y. Wu, J. Luo, Q. Zhang, M. Aleem, F. Fang, Z. Xue, and J. Cao. Potentials and challenges of phosphorus recovery as vivianite from wastewater: A review. *Chemosphere*, 226:246 – 258, 2019.
- [65] B. Örmeci and P.A. Vesilind. Development of an improved synthetic sludge: a possible surrogate for studying activated sludge dewatering characteristics. Water Research, 34(4):1069 – 1078, 2000.
- [66] Z. Čermáková, S. Švarcová, J. Hradilová, P. Bezdička, A. Lančok, V. Vašutová, J. Blažek, and D. Hradil. Temperature-related degradation and colour changes of historic paintings containing vivianite. Spectrochimica Acta Part A: Molecular and Biomolecular Spectroscopy, 140:101 – 110, 2015.

# **Appendix**

## A Tables and figures

Table A.1: Centrifugal experiment: TS and VS content of samples taken in triplicate from the feed, product and tailings. Sampled at three different splitter distances from the cylinder.

				TS in % v	wt	'	VS in % of	TS
Splitter distance in mm	Yield of sludge to product	Sample	Feed	Product	Tailings	Feed	Product	Tailings
		S1.1	4.61	4.17	4.11	65.49	69.90	70.51
1	98%	S1.2	4.65	4.27	3.88	65.66	70.64	71.80
		S1.3	4.68	4.19	3.99	65.71	71.43	72.32
		S2.1	4.57	4.27	4.08	67.48	70.41	70.37
0.75	86%	S2.2	4.56	4.33	3.88	67.20	70.41	71.73
		S2.3	4.52	4.43	3.86	67.24	69.93	70.58
		S3.1	4.77	4.28	4.38	65.04	70.82	70.25
0.25	80%	S3.2	4.75	4.33	4.11	66.48	70.41	69.11
		S3.3	4.84	4.36	4.05	65.32	70.11	69.88

Table A.2: Centrifugal experiment: TS and VS content of samples taken without centrifuging and while centrifuging, without splitting. Including Fe and P content determined by ICP-OES analysis.

	Sample	Total solids in % wt	Volatile solids in % of TS	ICP-OES Sample	Fe (mg/g ds)	P (mg/g ds)
	1	3.95	65.16	1	58.68	30.14
Without	2	3.96	65.73			
centrifuging	3	4.17	65.89			
	4	4.56	70.25			
	1	3.52	69.85	1	44.98	26.53
	2	3.48	70.26	2	46.04	26.85
While	3	3.67	70.81			
centrifuging	4	3.64	71.38			
	5	3.57	71.56			
	6	3.73	70.74			
	7	3.66	72.53			

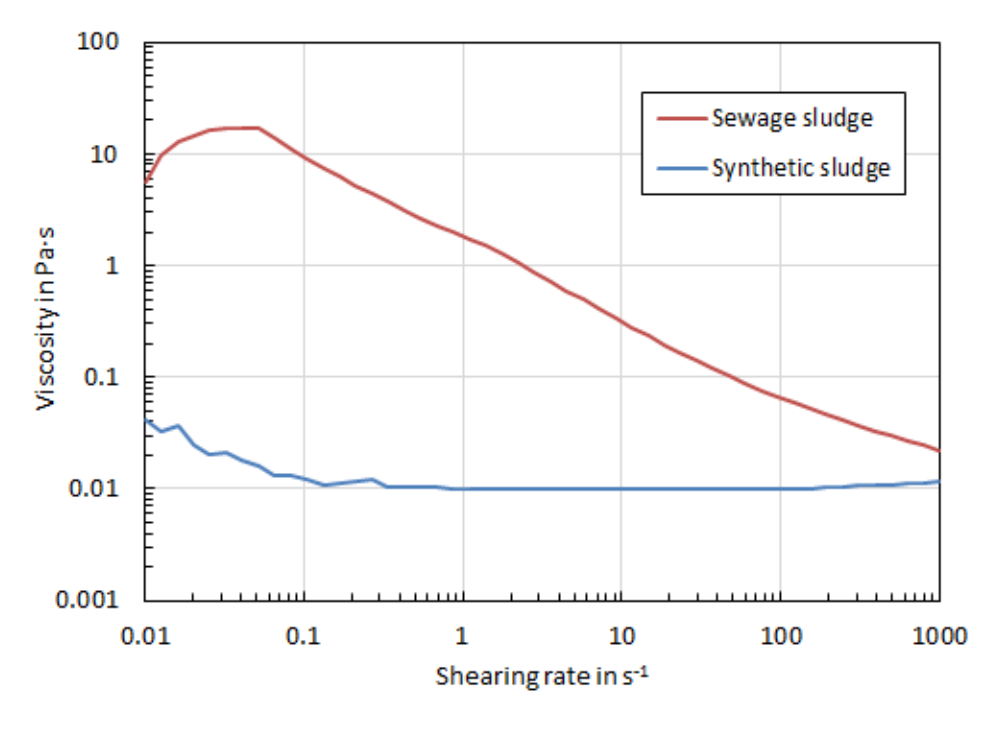


Figure A.1: Viscosity curves for synthetic and sewage sludge.

## **B** Photos and images



Figure B.1: Connection of cylinder to drill with two plates.



Figure B.2: The closed-loop spiral setup.

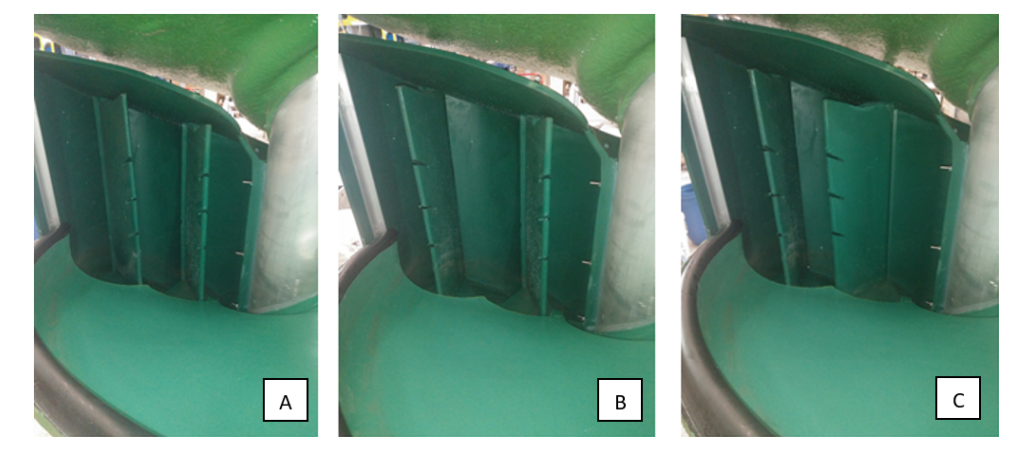


Figure B.3: Photos of the splitter configurations.

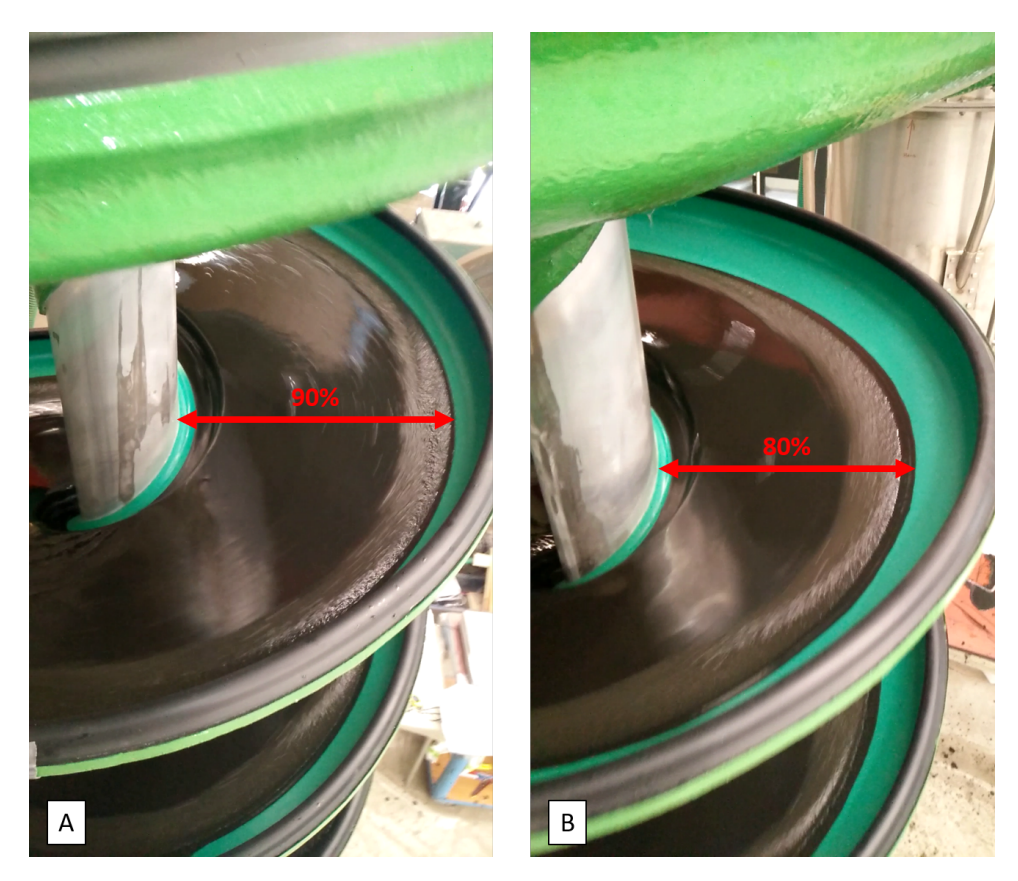


Figure B.4: A: Sludge flow before the repulper covering 90% of the trough. B: Sludge flow after the repulper covering 80% of the trough.



Figure B.5: Slow-moving bed of sand near the column in 20% diluted sludge.



Figure B.6: Map of the Netherlands showing all sewage treatment plant locations[52].